Geochemistry, Geophysics, Geosystems®

AGU ADVANCING EARTH AND SPACE SCIENCE

RESEARCH ARTICLE
10.1029/2021GC010030

Key Points:

- We classify a new mafic magmatic province buried beneath the Northwest Shelf of Australia
- Classification was achieved by implementing a 3D seismic stratigraphic model and integrating geophysical and geochemical findings
- Implications include new resource opportunities, potential contributions to end Permian mass extinction and large scale CO_2 sequestration

Correspondence to:
C. T. G. Yule,
christopher.yule@my.jcu.edu.au

Citation:
Yule, C. T. G., & Spandler, C. (2022). Geophysical and geochemical evidence for a new mafic magmatic province within the Northwest Shelf of Australia. *Geochemistry, Geophysics, Geosystems*, *23*, e2021GC010030. https://doi.org/10.1029/2021GC010030

Received 15 JUL 2021
Accepted 14 OCT 2021

Author Contributions:
Conceptualization: C. T. G. Yule, C. Spandler
Data curation: C. T. G. Yule, C. Spandler
Formal analysis: C. T. G. Yule, C. Spandler
Investigation: C. T. G. Yule, C. Spandler
Methodology: C. T. G. Yule, C. Spandler
Resources: C. T. G. Yule, C. Spandler
Supervision: C. Spandler
Validation: C. Spandler
Writing – review & editing: C. Spandler

Geophysical and Geochemical Evidence for a New Mafic Magmatic Province Within the Northwest Shelf of Australia

C. T. G. Yule[1] and C. Spandler[2]

[1]Department of Earth and Environmental Sciences, James Cook University, Townsville, Australia, [2]School of Physical Sciences, The University of Adelaide, Adelaide, Australia

Abstract The formation of mafic magmatic provinces are significant geological events that can drive mass extinctions and continental rifting and can influence basin evolution, petroleum prospectivity and mineralization. Buried magmatic provinces, however, are rarely identified and difficult to define. The Northwest Shelf of Australia contains large volumes of potentially interconnected mafic igneous material across several sedimentary basins. However, limited study and a lack of surface exposure have prevented detailed description and classification of these rocks. In this study, the distribution and composition of these mafic igneous rocks are described using an integrated geophysical and geochemical approach, which included over 10,000 km line length of 2D seismic data, well log data and chemical analysis of samples from 14 wells across the Browse, Roebuck, Canning and North Carnarvon basins. Using this combined data set, we demonstrate interconnectivity of buried mafic igneous rocks across the Northwest Shelf and calculate a total surface area exceeding 280,000 km^2 and a cumulative minimum volume of ~140,000 km^3. Petrology and geochemistry of samples indicate they are basaltic and doleritic with alkaline and sub-alkaline compositions and formed in a continental rift setting. Collectively, the igneous rocks meet the criteria for classification as a mafic magmatic province (MMP) and closely match the criteria required for classification as a large igneous province (LIP). Emplacement of the newly defined Northwest Shelf MMP may represent hotspot magmatism that could have initiated rifting of the Cimmerian Block from NW Australia during the Permian and could have potential for future, large scale CO_2 sequestration and storage.

Plain Language Summary Magmatic provinces are large bodies of igneous rock often tied to significant changes in Earth's history such as mass extinction events and continental rifting. Many magmatic provinces are exposed on the surface and can be studied directly; however, studying magmatic provinces that are buried under hundreds to thousands of meters of sedimentary rock becomes increasingly difficult. In this paper, we indirectly map and characterize igneous rocks buried within the Northwest Shelf of Australia using seismic data and drilled rock samples. Combining these results, we found the igneous rocks all formed together, most likely during supercontinent break-up around 250 million years ago. We conclude that these rocks represent a new magmatic province, named the Northwest Shelf Mafic Magmatic Province. Recognition of this magmatic province is exciting because it may have contributed to an important global extinction event, presents new mineral resource opportunities and may be suitable for large scale CO_2 sequestration to combat climate change.

1. Introduction

The emplacement or eruption of large volumes of mafic magma over relatively short timescales is well recognised as important geological phenomena that has influenced mass extinctions, continental breakup, and metalliferous ore formation across Earth's history (Ernst, 2014). The most voluminous of these events, classified as Large Igneous Provinces (LIPs), are characterized by extensive flood basalts associated with dolerite dyke and sill networks that are genetically related to a mantle plume, and/or continental break-up geodynamics (Ernst et al., 2005). To classify a LIP, a mafic igneous suite must cover an area of at least 100,000 km^2, have a minimum volume of 100,000 km^3 and be emplaced within a 50-million-year time period (Coffin & Eldholm, 1994; Ernst & Buchan, 2001; Ernst et al., 2005). An episode of mafic magmatism that meets some, but not all, of these requirements can be classified as a Mafic Magmatic Province (MMP) rather than a LIP, given the same surface area and volume requirements are met (Ernst, 2014).

Historically, most LIPs have been classified primarily on exposed extrusive components, although characterizing pre-Mesozoic magmatic provinces, even when exposed at Earth's surface, can be challenging due to the high tendency of mafic igneous rocks to weathering and erosion (Wingate et al., 2004; Xu et al., 2014). Identifying buried mafic igneous rocks within sedimentary basins is also challenging due to the lack of surface exposure and access to rocks samples (Eide et al., 2017; Schofield et al., 2017). Therefore, it is likely that the number of recognised LIPs and MMPs within ancient sedimentary basins is underestimated. Nevertheless, the emplacement of LIPs or MMPs into basins may have important implications for basin formation and evolution, and for global climate. Basin evolution can be controlled by uplift during igneous emplacement, followed by increased subsidence as the igneous units cool (Houseman, 1991; Pirajno & Santosh, 2015; Zeyen et al., 1997). Continental break-up, which is known to correlate with LIP emplacement (Ernst et al., 2005; Glass & Phillips, 2006; Kravchinsky, 2012; Wingate et al., 2004), can affect basement structures, leading to the further development of sedimentary depocenters (Ernst et al., 2005; Müller et al., 2005). Hydrocarbon systems can be severely impacted by magmatic intrusions. The additional heat can thermally mature source material into the oil window, and igneous rocks can form effective seals (Schutter, 2003; Totterdell et al., 2014). Conversely, intrusions can thermally decay source material and compartmentalize reservoirs which restricts hydrocarbon migration (Augland et al., 2019; Black & Gibson, 2019). Thermal and/or mechanical modification to hydrocarbons and sedimentary host rocks can release significant volumes of greenhouse gasses into the atmosphere causing disruptions to the global climate and global mass extinctions, such as the end-Permian mass extinction event caused by a LIP (Augland et al., 2019; Burgess et al., 2017; Ernst et al., 2005; Glass & Phillips, 2006; Kravchinsky, 2012; Wingate et al., 2004). LIPs and MMPs are also known to host significant orthomagmatic Ni-Cu-platinum group element (PGE) deposits (Wingate et al., 2004) and, hence, are targeted for mineral exploration.

Mafic igneous rocks have been reported from sedimentary basins across the Northwest Shelf of Australia, identified primarily from hydrocarbon exploration data (Table 1). Igneous rocks are often overlooked or avoided during hydrocarbon exploration (Kutovaya et al., 2019; Schutter, 2003) and no outcrop of these igneous rocks has yet been identified from the region. Few studies have investigated these units specifically, so they remain poorly understood. Recent studies by Rohrman (2013) Magee et al. (2016), Eide et al. (2017), Schofield et al. (2017), MacNeill et al. (2018), Rollet et al. (2019) and Magee and Jackson (2020) used geophysical techniques (i.e., seismic, gravity and magnetics) to estimate the thickness and distribution of igneous units in the sedimentary basins of the Northwest Shelf. Initially proposed by Symonds et al. (1998) and later suggested by MacNeill et al. (2018), the igneous units emplaced within these basins may constitute a mafic magmatic province (MMP), while Rollet et al. (2019) proposes the presence a large igneous province (LIP). However, no previous work has been able to demonstrate that the igneous units fully meet the criteria of a magmatic province.

Geophysical techniques are the primary means of imaging and understanding subsurface geology at a broad (>1 km) scale. Of these, reflection seismic surveying is the only method for imaging geological features with a reasonable resolution and for estimating lithologies several km below the surface (Yilmaz, 2001). Nevertheless, like most geophysical techniques, inversion of reflection seismic signals requires lithological inputs (Austin et al., 2014), which may lead to ambiguous results if the lithology is poorly known (Luke et al., 2003; Yilmaz, 2001). Hence, optimal results are obtained when geophysical interpretations are integrated with geological and geochemical data. In this study, reflection seismic interpretations are supported by geological context and geochemical datasets, which together provide robust constraints on the extent, composition, and tectonic setting of the mafic igneous units.

To investigate the hypothesized presence of a LIP or MMP buried across the Northwest Shelf of Australia, we integrated over 10,000 km line length of 2D seismic data and 24 well logs (Figure 1a) into a single 3D model. This model was used to map the distribution and interconnectivity of mafic igneous units across four basins of the Northwest Shelf. Furthermore, we studied 24 rock samples from 14 different exploration wells (Table 1) for their petrography and bulk geochemical composition to shed light on the origins and composition of these mafic units. Identification of a LIP or MMP in the Northwest Shelf of Australia is not only important for understanding basin evolution, but also has implications for assessment of hydrocarbon (Augland et al., 2019; Black & Gibson, 2019) and Ni-Cu-PGE mineralization (Wingate et al., 2004) potential in the region, as well as targeting of CO_2 sequestration projects (e.g., Goldberg et al., 2008). The broader application of the integrated geophysical and geochemical approach used in this study may aid in the discovery of similar features that remain hidden in other basins worldwide.

Table 1
Well Report Information of Mafic Igneous Rock Sampled and Geochemically Analyzed in This Study

					Emplaced formation		
Sample name	Sample type	Depth (m)	Lithology	Previous dates (Ma)	Name	Lithology	Period
Bedout 1	Core	3,042.5	Basalt	–	?	Sandstone	Early Triassic
Corbett 1	Cuttings	332	Dolerite	–	Liveringa Group	Sandstone, siltstone	Permian
Fraser River 1	Core	3,069.3	Dolerite	163 ± 13 (Fission track)	Fairfield Group	Limestone, shale	Early Carboniferous
Hannover South 1	Cuttings	5,200	Mafic volcanics	–	Keraudren Formation	Sandstone	Triassic
Hannover South 2	Cuttings	5,300	Mafic volcanics	–	Keraudren Formation	Sandstone	Triassic
Hannover South 3	Cuttings	5,400	Mafic volcanics	–	Keraudren Formation	Sandstone	Triassic
Hauy 1	Core	821.7	Basic igneous	–	?	Sandstone	Triassic
Lagrange 1	Cuttings	3,245	Bedout volcanics	253 ± 3 (K-Ar)	Keraudren Formation	Sandstone	Triassic
Minjin 1	Cuttings	1,415	Dolerite	–	Grant Group	Sandstone	Permian
Moogana 1	Cuttings	2,165	Metadolerite	–	Pillara Formation	Limestone	Devonian
Padilpa 1	Cuttings	1,987	Dolerite	336 ± 2 (K-Ar)	Fairfield Group	Limestone, shale	Early Carboniferous
Padilpa 2	Cuttings	2,174	Dolerite	336 ± 2 (K-Ar)	Fairfield Group	Limestone, shale	Early Carboniferous
Padilpa 3	Core	1,815	Dolerite	336 ± 2 (K-Ar)	Fairfield Group	Limestone, shale	Early Carboniferous
Pearl 1A	Cuttings	2,037.5	Dolerite	249 ± 2 (K-Ar)	?	Shale/Siltstone	Early Carboniferous
Pearl 1B	Cuttings	2,037.5	Dolerite	249 ± 2 (K-Ar)	?	Shale/Siltstone	Early Carboniferous
Pearl 2	Cuttings	2,185	Dolerite	249 ± 2 (K-Ar)	?	Shale/Siltstone	Early Carboniferous
Perindi 1	Cuttings	1,590	Dolerite	291 ± 2 (K-Ar)	Grant Group	Sandstone	Permian
SD 1	Core	693.2	Dolerite	224.19 ± 2.95 (Ar-Ar)	Noonkanbah Formation	Mudstone, siltstone	Permian
SD 2	Core	675.55	Dolerite	–	Noonkanbah Formation	Mudstone, siltstone	Permian
Tappers Inlet 1	Core	2,855.4	Metabasalt	–	Nambeet Formation	Sandstone	Ordovician
Wamac 1	Cuttings	2,250	Dolerite	–	Anderson Formation	Sandstone	Early Carboniferous
Wamac 2	Cuttings	2,375	Dolerite	228 ± 5 (K-Ar)	Anderson Formation	Sandstone	Early Carboniferous
Wamac 3	Cuttings	2,675	Dolerite	–	Anderson Formation	Sandstone	Early Carboniferous
Wamac 4	Cuttings	2,725	Dolerite	–	Anderson Formation	Sandstone	Early Carboniferous

Note. Information includes sample depth and lithology, dates from previous studies and well reports (see Section 2.3.2), and sedimentary units the mafic igneous rocks were emplaced in NOPIMS (2019), WAPIMS (2019). The lithologies included in this table are as described from the well reports. Note, sample names differ to well names as all well names end in 1. Well completion reports can be found as links to NOPIMS in the supplementary materials in Yule & Spandler (2021). Well completion reports for onshore wells can be found in the WAPIMS Database (https://wapims.dmp.wa.gov.au/WAPIMS/).

2. Geological Background

Australia's Northwest Shelf region is a passive margin consisting of several Paleozoic-Mesozoic basins that range in thickness from 1 to 18 km. The region itself covers >1,500,000 km^2 (Figure 1b) and is renowned for hosting Australia's richest hydrocarbon resources (Totterdell et al., 2014). These basins include (north to south) the Browse, Roebuck, Canning, and North Carnarvon Basins. Major hydrocarbon resources are found in the North Carnarvon and Browse Basins (Blevin et al., 1994, 1998; Hackney et al., 2015), and minor hydrocarbon discoveries have been identified in the intervening Canning and Roebuck Basins (Figure 1a; Totterdell et al., 2014). Extensive hydrocarbon exploration means the Cenozoic and Mesozoic geological history is well understood across these basins. However, the Paleozoic stratigraphy is frequently underrepresented because overlying igneous rocks obscure deep seismic imaging (Mory & Haines, 2013; Totterdell et al., 2014). The basins of the Northwest Shelf host Paleozoic and Mesozoic strata that record a rich geological history, characterized by several regional tectonic events.

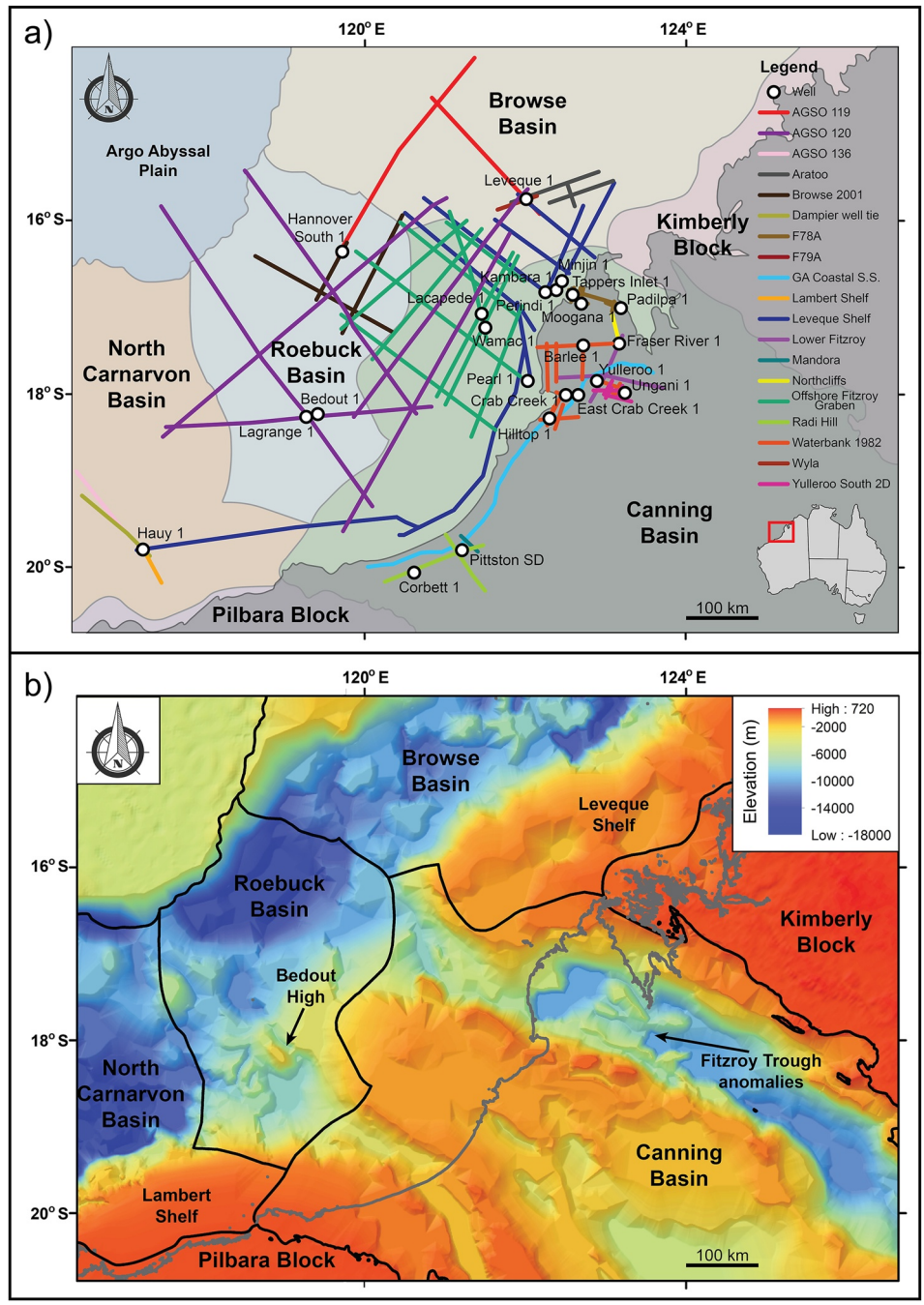

Figure 1. (a) Northwest Shelf study area and locations of seismic and well data used. All featured wells were used for seismic stratigraphic mapping, whereas only some wells were sampled for geochemical analyses (see Supplementary Material Supporting Tables in Yule & Spandler, 2021). (b) Basement map of the study area, which was compiled from magnetics, gravity, geological and well data by Frogtech (2014). Basement elevation is an approximation and can by be influenced by, for example, mafic igneous rocks.

2.1. Tectonic History

The tectonic development of the Northwest Shelf can be broadly characterized by three episodes of continental rifting. (a) During the Cambrian, the Tarim Block rifted from the Northwest Shelf region in a north-westerly direction and later coalesced to become part of what is now the Xinjiang Province in north-western China (Keep et al., 2007; Li et al., 2008; Li & Powell, 2001; Merdith et al., 2021). This event led to the onset of subsidence and

sedimentation in the oldest basin in the region, the Canning Basin. (b) Permian rifting of the Cimmerian Block, a group of continental fragments that formed during the Devonian and were part of the northern Gondwana margin (Li et al., 2008). This rifting event, referred to as the Bedout Movement (Müller et al., 2005), was likely initiated by impingement of a mantle plume beneath the continental lithosphere resulting in the formation of a tectonic triple junction, a raised basement structure in the Roebuck Basin called the Bedout High, and a regional unconformity (MacNeill et al., 2018; Müller et al., 2005; Rohrman & Lisk, 2010; Rollet et al., 2019). (c) Northward rifting of the Mawgyi Terrane at ca. 155 Ma in the Jurassic, initiated further subsidence across the Northwest Shelf. This rifting event resulted in the formation of the Argo Abyssal Plain, the oceanic crust adjacent to the Northwest Shelf (Heirtzler et al., 1978; Metcalfe, 2006; Müller et al., 2005; Yeates et al., 1984). Lastly, throughout the Cenozoic, the Northwest Shelf has existed as a passive margin subject to mild north-south compression as the Australia plate moves northward into the Banda arc (DiCaprio et al., 2009; Keep et al., 2007).

2.2. Basins

2.2.1. Browse Basin

The Browse Basin (Figure 1) is an offshore, petroleum producing basin that represents a significant portion of Northwest Shelf's depositional history (Geoscience Australia, 2019). Strata within the Browse Basin is dominated by sandstones from the Carboniferous to Middle Jurassic, claystones from the Middle Jurassic to Upper Cretaceous and limestones throughout the Cenozoic. Sedimentation initiated during the early Carboniferous as half-graben extensional structures. A series of rifting and subsidence events throughout the Paleozoic and Mesozoic facilitated the development of significant depocenters, the thickest of which is up to 15 km (Nicoll et al., 2009).

2.2.2. Roebuck Basin

Formation of the Roebuck Basin (Figure 1) is attributed to multiple phases of rifting throughout the Paleozoic and Mesozoic and from thermal sag in the Triassic (Totterdell et al., 2014). The Roebuck Basin is dominated by limestone, mudstone and siltstone that first deposited in the Middle Devonian but are thickest in the Mesozoic intervals. Although sediment thickness is up to 6 km, a basaltic lava delta with a maximum estimated thickness of 10 km has been recognised along the continental shelf edge (Rollet et al., 2019). The Roebuck Basin is also partly defined by the Bedout High, a basement high in the Bedout Sub-basin that is capped by basalt and appears as a major anomaly in potential field. The Roebuck Basin is a frontier petroleum basin that is understudied but is recognised to contain significant quantities of igneous material (Müller et al., 2005; Totterdell et al., 2014).

2.2.3. North Carnarvon Basin

Most units in the North Carnarvon Basin (Figure 1) consist of sandstones, siltstones, claystones, limestones and marls. Sedimentation initiated in the early Carboniferous due to continental rifting, but widespread sediment deposition did not occur until the late Permian–Early Triassic when all the basin elements developed. Depocenters formed by rifting and subsidence that created thick sedimentary packages up to 15 km thick. Hosted in some sedimentary units are basalts, but detailed mapping is limited, and their extent is not fully understood (McClay et al., 2013). Despite the presence of igneous rocks, the North Carnarvon Basin is Australia's largest producer of hydrocarbon resources and contains a complex stratigraphy that requires further exploration (Geoscience Australia, 2019).

2.2.4. Canning Basin

The Canning Basin is divided into onshore and offshore components (Figure 1). Near continuous deposition from Ordovician to present has produced thick, mostly Paleozoic stratigraphic packages, including the regionally extensive and up to 2,500 m thick Grant Group (Smith et al., 2013; Totterdell et al., 2014; Yeates et al., 1984). These packages contain a variety of sedimentary rocks including limestone, sandstone, mudstone and siltstone. A tectonic history of crustal sag, subsidence and continental rifting has produced one of the largest depocenters in the Northwest Shelf that contains up to 18 km of strata. Within the strata are basalt flows and dolerite dykes and sills. The Canning Basin is a vast, frontier basin that lacks well control and preserves much of the geological record that is missing from other areas (e.g., the Silurian; Brown et al., 1984; Totterdell et al., 2014).

2.3. Mafic Igneous Rocks

Mafic igneous units are known to extend from the Carnarvon Basin in the south, throughout the Canning and Roebuck basins and north into the Browse Basin (MacNeill et al., 2018; Magee & Jackson, 2020; Rohrman, 2013; Rohrman & Lisk, 2010; Rollet et al., 2019; Symonds et al., 1998). The maximum thickness of these rocks is ~10 km along the continental shelf edge of the Roebuck Basin, and is associated with a lava delta. This measurement is based on seismic, magnetic and gravity data (MacNeill et al., 2018; Rollet et al., 2019) but the igneous units thin toward the Canning Basin. The main challenge of investigating these mafic igneous rocks is that they are only known from sparse drill core and cuttings from hydrocarbon exploration wells (Table 1) and geophysical observations (Totterdell et al., 2014). A better understanding of the nature and extent of these magmatic intrusions is crucial because they are a critical risk to petroleum prospectivity across the Northwest Shelf, particularly with respect to over-maturation from thermal decomposition (Augland et al., 2019; Black & Gibson, 2019; Holford et al., 2013; Smith et al., 1999; Totterdell et al., 2014).

2.3.1. Geophysics

Using seismic data, Symonds et al. (1998) was the first to propose that mafic igneous rocks along the Northwest Shelf may constitute a magmatic province. MacNeill et al. (2018) later identified over 100,000 km^2 of mafic igneous rocks up to 10 km thick in the Roebuck Basin using 2D and 3D seismic data. The most recent study of mafic units in the Northwest Shelf was that of Rollet et al. (2019), who combined regional gravity and magnetic surveys with seismic data to map the extent of the mafic units along the offshore margin. Findings from this study support the previous thickness estimate of 10 km by MacNeill et al. (2018) but also used changes in calculated rock density through vertical sections to map the distribution of the mafic units. This work was the first to comprehensively demonstrate the mafic units are interconnected. The size of the mafic units suggests a buried LIP that formed during the late Permian-Early Triassic as determined by stratigraphic relationships.

2.3.2. Radiometric Geochronology

Previous geochronological studies of mafic igneous units in the study area (Figure 1) employed fission track and $^{40}K/^{39}Ar$ geochronology on rocks from six well samples in the Canning Basin (Gleadow & Duddy, 1984; Reeckmann & Mebberson, 1984). Fission track dating of apatite indicates a thermal event occurred at ~270 Ma in the middle Permian (Gleadow & Duddy, 1984), whereas $^{40}K/^{39}Ar$ data suggests mafic igneous rocks were emplaced between early Permian and Jurassic (~291 Ma to ~176 Ma), but are likely Permian in age (Reeckmann & Mebberson, 1984). These dates have been crucial for providing broad constraint on the emplacement of these igneous rocks, but more precise geochronology is required to confidently correlate the emplacement of these rocks with geological events such as the continental break-up of the Cimmerian Block in the Permian (Mory & Haines, 2013). Additionally, relative dating of the nearby Exmouth Plateau LIP suggests a Jurassic emplacement (Magee & Jackson, 2020; Rohrman, 2013). Although the Exmouth LIP and igneous units from this study are separate, a Jurassic emplacement age should be considered until more radioisotope geochronology data is acquired.

2.3.3. Geochemistry

The mineralogical and chemical composition of the mafic igneous units found across the Northwest Shelf is poorly understood, most likely due to the highly restricted availability of rock samples as expressed in the NOPIMS and WAPIMS databases. The only investigation of the chemical composition of these rocks is a data set acquired by Chemostrat (2016) involving four basalt samples from the Bedout 1 well with no interpretations accompanying the data. No previous studies have addressed the geochemistry or mineralogy of mafic igneous rocks on a regional scale. The primary impediment to geochemical investigations is the deep emplacement of mafic igneous units where sample collection is restricted to a handful of hydrocarbon exploration wells. Well samples vary between drill core and cuttings (Table 1), but cuttings present contamination issues from material up well, and the few core samples that are available are strongly geochemically altered.

3. Methods

3.1. Seismic Interpretations

The geophysical approach of this study integrated 24 well logs and over 10,000 km line length of 2D seismic data (Figure 1) into a regional 3D model. Well logs contain lithological data that is crucial for seismic

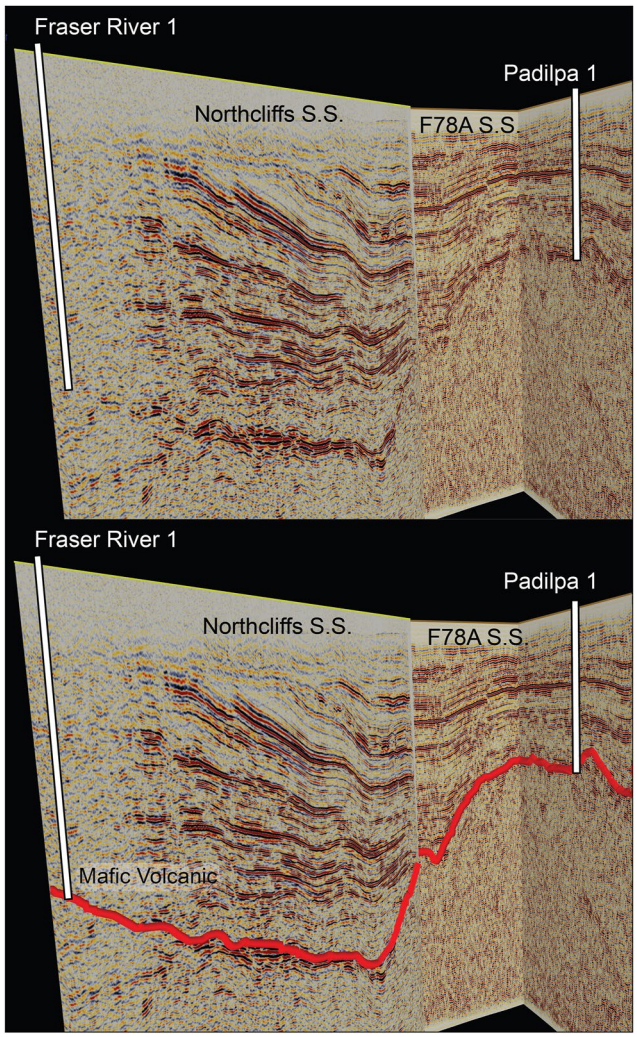

Figure 2. Illustration of how the top reflector of mafic igneous rocks are mapped in seismic data by linking well lithology logs that are tied using a synthetic seismogram. The wells in this illustration are Fraser River 1 and Padilpa 1. The lower boundary of mafic igneous rocks are ambiguous and could not be mapped due to strong attenuation.

stratigraphic mapping, but some wells also have geophysical logs such as gamma, density, resistivity and sonic logs, which can assist in differentiating rock types. The wells and seismic lines were analyzed in 3D space using the OpendTect software package to map the extent of the buried mafic igneous units across the study area (Yule & Daniell, 2018, 2019). Mafic igneous units are typically expressed as high-amplitude seismic reflections relative to the surrounding sedimentary rocks and appear as three types: flows, dykes and sills (Magee & Jackson, 2020). Flows are emplaced above older strata whereas dykes and sills crosscut them. Dykes orient vertical to sub-vertical to the bedding plane and disrupt seismic signal and sills have a stratiform orientation (Magee & Jackson, 2020; Phillips et al., 2018). Strong magnetic signals can differentiate mafic units from other geological units, which is useful for seismic stratigraphic mapping (Cortez & Cetale Santos, 2016; Eide et al., 2017; Sun et al., 2010). Mapping involved laterally tracing high amplitude seismic reflectors between well logs that intersected mafic igneous rocks and using published seismic interpretations (AGSO, 2001; Hashimoto et al., 2018; Rollet et al., 2019) to create 2D horizons (Figure 2; see Supplementary Materials A in Yule & Spandler, 2021). The 2D mafic igneous horizons were imported into Generic Mapping Tools (GMT) to be interpolated into 3D surfaces. After testing a variety of interpolation functions and parameters including nearest neighbor and triangulation, a spline with a tension factor of 0.75 was the optimal function as it produced a smooth and consistent surface. The interpolated surface was then imported to R to create a boundary using the concaveman function to remove data outside the extent of the seismic lines (see Supplementary Materials B in Yule & Spandler, 2021). The result is a continuous 3D surface generated from seismic and well data that displays the location and depth of the mafic igneous rocks across the study area (Figure 3). Using this 3D surface and estimates of mafic igneous rock thickness across the study area (MacNeill et al., 2018; Rollet et al., 2019), a volume of magmatic material was calculated.

3.2. Mafic Rock Sample Analysis

Sampling of igneous rocks is hampered in the study area due to the lack of surface exposure and well control in these frontier basins. Well density in the offshore Canning Basin is 0.8/10,000 km^2, which is >500 times less than, for example, North American Paleozoic basins (Cadman et al., 1993; GSWA, 2017). These differences in well density shows a data disparity in large areas of the Northwest Shelf. Thus, the approach to sampling in this study was to sample as many wells that contained mafic igneous material as possible. Some of the wells displayed in Figure 1 did not have enough material for analysis (less than 30 grams), so the wells listed in Table 1 represent the most comprehensive sampling for mafic igneous units in the study area.

The well samples consist of drill core and drill cuttings (see Supplementary Materials Supporting Tables in Yule & Spandler, 2021). Pieces of core were made into standard thin sections and epoxy pucks for textural analysis and mineral identification using a petrographic microscope and an energy dispersive spectrometer-equipped scanning electron microscope (SEM-EDS) (see Supplementary Materials C in Yule & Spandler, 2021) at the Advanced Analytical Center, James Cook University, Townsville, Australia. The cuttings were thoroughly cleaned using a sonic bath to remove drilling mud and organic matter, then both core and cuttings were crushed to <500 μm using a tungsten-carbide disc mill. The crushed samples were submitted to Bureau Veritas Minerals laboratories, Vancouver, Canada, where they were milled and then analyzed for major and trace elements using a combination of inductively coupled plasma mass spectroscopy (ICP-MS) and inductively coupled plasma optical emission spectroscopy (ICP-OES). More detail on these methods are described by Slezak and Spandler (2020). Full analytical results are presented in Supplementary Materials D in Yule & Spandler (2021).

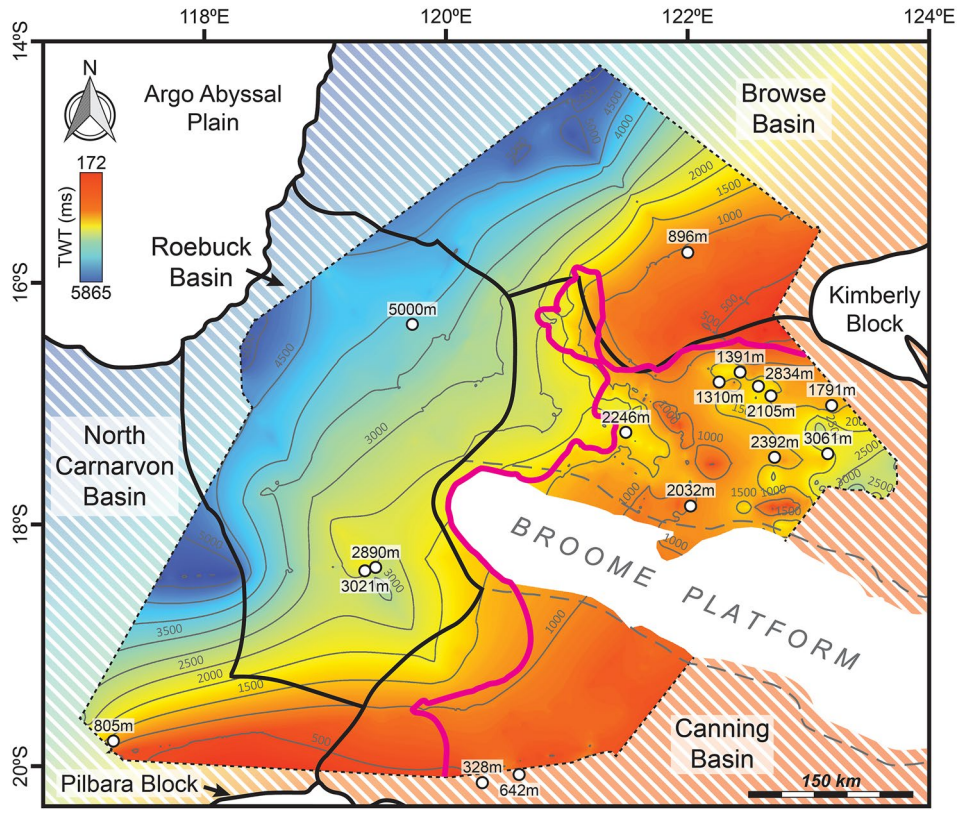

Figure 3. Top of the mafic magmatic province (MMP) across the Northwest Shelf, covering ~280,000 km^2 across four basins. Contours are labeled in milliseconds two-way travel time (TWT) and wells that intersect the MMP are labeled with depth in meters from the rotary table. Not all wells from Figure 1 were used because some wells only reported contact metamorphism from lower intrusions or did not intercept igneous units. Striped areas are possible locations of the MMP but were out of scope for this study. The purple line represents an approximate change in lithology where northwest of the line is interpreted as extrusive basalt and southeast is intrusive dolerite based on stratigraphic relationships shown in Figure 11.

Bulk mineralogy of the samples was determined using X-ray diffraction (XRD) at the North-West University Center for Water Science and Management laboratory, Potchefstroom, South Africa. XRD data were collected using a PANalytical X'Pert Pro with a Cu X-ray anode (Kα) that measures diffraction angles from 4° to 100° (see Supplementary Materials D in Yule & Spandler, 2021).

4. Results

4.1. Seismic Correlation

The igneous units show a surprising level of connectivity in the seismic data. Mapping from well to well, the mafic igneous rocks are found throughout the study area, except on the Broome Platform in the Canning Basin (Figure 3). Igneous horizons are found from the eastern edge of the North Carnarvon Basin through to the Southern area of the Browse Basin and are continuous across the onshore-offshore transition in the Fitzroy Trough/Oobagooma and Willara Sub-basins (see Supplementary Material A in Yule & Spandler, 2021). There is also a general stratigraphic trend where the igneous units are above the early Permian Grant Group outside the Canning Basin, but are underneath the Grant Group in the Canning Basin (Figure 3).

In this study, the mafic rocks are expressed as two types: intrusions that cross-cut Paleozoic strata or as lava flows overlain by Triassic strata (Table 1; see Supplementary Material A in Yule & Spandler, 2021). These two types are expressed in seismic data where intrusions appear as high amplitude reflectors that cut across and influence other reflections (Figure 4a), whereas lava flows generally conform with adjacent strata but can be differentiated by higher amplitudes (Figure 4b). Additional well control in the form of thin-section petrography highlights the intrusions are fine-to medium-grained dolerites, and the lava flows are basalts (Section 4.2).

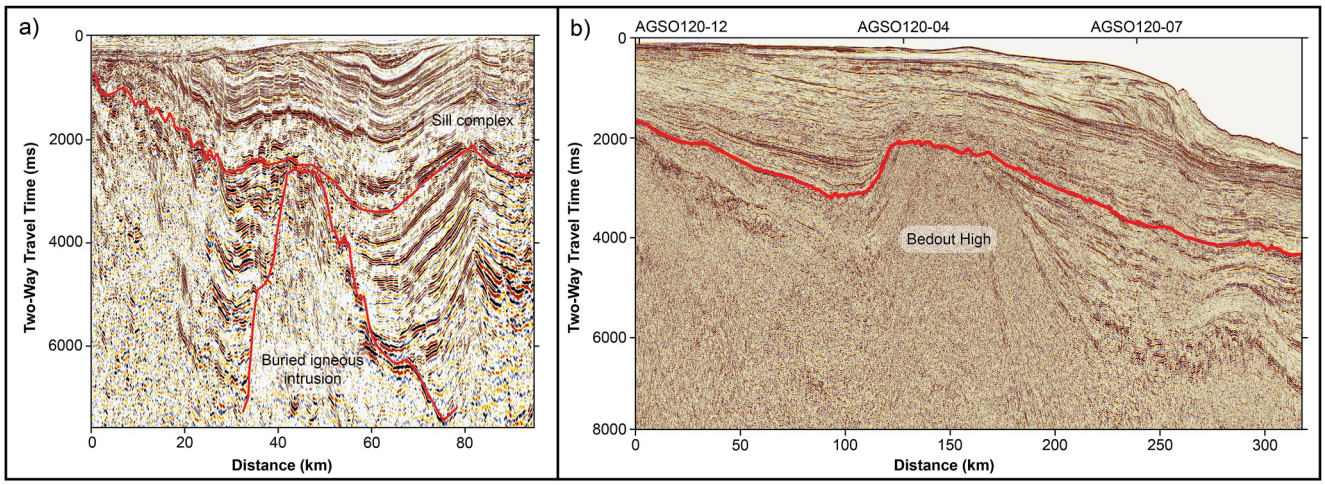

Figure 4. (a) Igneous intrusion imaged in GA Coastal S.S. measuring at ~40 km across the base and ~5,000 milliseconds (TWT) in height. The red line above the intrusion is interpreted as the top of the MMP. (b) Bedout High in seismic data as imaged in AGSO120 M.S.S. in line 01. It is approximately 150 km in diameter and more than 4,000 milliseconds (TWT) in height. The red line is interpreted as the top of the MMP.

Figure 3 represents the top of either type of igneous unit by interpolating 2D seismic horizons. The calculated minimum and maximum depths are 172 and 5,918 ms two-way travel time (TWT). The depth of the igneous rocks is as shallow as 300 m onshore and becomes steadily deeper offshore trending NW, but there are anomalies to this trend. The igneous units are found deeper in the Fitzroy Trough/Oobagooma Sub-basin of the Canning Basin than in the adjacent Willara Sub-basin and Browse Basin (Figure 3) and the center of the Fitzroy Trough contains ~4,000 ms tall intrusions (Buried volcanic intrusion: Figure 4a) that are visible on the basement map (Fitzroy Trough anomalies: Figure 1b). The other major anomaly is the Bedout High (Figure 4b) in the Roebuck Basin, which is a structural high with volcanic origins, as indicated by wells Bedout 1 and Lagrange 1 where the latter intersected over 300 m of basalt into the structure (Table 1). It appears that basalt was emplaced over the Bedout High as expressed in the seismic data (Figure 4b; see Supplementary Material A in Yule & Spandler, 2021), which resulted in a depth anomaly in the interpolated horizon (Figure 3).

The total area covered by mafic igneous units from seismic stratigraphic mapping is ~280,000 km^2 (Figure 3). The surface area was calculated by importing the interpolatedhorizon of mafic igneous rock into ArcGIS with the same coordinate system as OpenDtect (WGS84, UTM 51S) and running a surface area query. The value of ~280,000 km^2 is regarded as the minimum surface area because it is likely that the igneous units extend further outside the study area. To better understand the surface area of the igneous units, further improvements to the interpolated seismic model can be made with targeted seismic surveys and new wells to ground-truth the interpretations presented within this study.

4.2. Mineralogy and Petrography

The dolerite samples analyzed in thin sections (Figure 5), SEM-EDS (Figure 5) and XRD (Figure 6) (see Supplementary Materials C and D in Yule & Spandler, 2021) have typical doleritic textures with lathic plagioclase typically 0.5–2 mm long (50%–70%), pyroxene (mostly clinopyroxene; up to 40%), magnetite (5%) and alteration phases such as quartz, calcite, chlorite and sulfides (up to 20%) (Figures 5 and 6). Several samples are porphyritic with plagioclase phenocrysts up to 5 mm in length. The basaltic samples are fine grained with plagioclase, pyroxene, quartz and magnetite grains visible from petrographic examination (Figure 5), but these samples are also heavily altered (up to 60%) with the same alteration phases as the dolerites. All thin section samples are strongly magnetic.

Primary magmatic phases include plagioclase, pyroxene and magnetite, and accessory ilmenite and titanite, and alteration phases include quartz, calcite, chlorite, pyrite, chalcopyrite and K-feldspar (Table 2). Olivine is preserved in some samples but is rare due to its susceptibility to alteration (Figures 5a and 5b). Three abundant types of alteration in these samples are chloritic, carbonate and silicic alteration (Figures 5c–5f). Chloritic

10.1029/2021GC010030

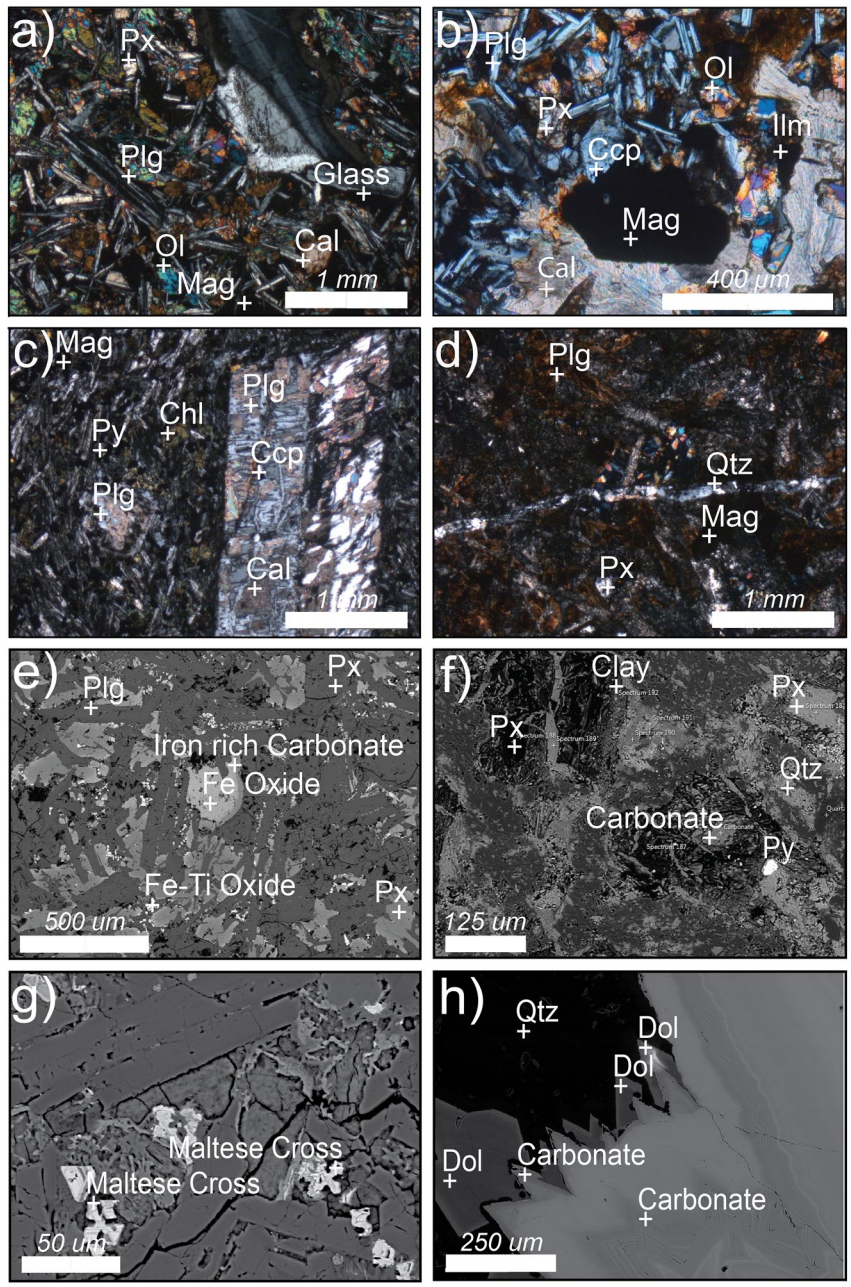

Figure 5. Thin section petrography under cross-polarised (XPL) light and SEM-EDS analysis of samples. (a) SD2, the freshest dolerite in this study under XPL. (b) SD1 under XPL, is abundant in magnetite, lathic plagioclase and calcite. (c) Bedout 1 shown in XPL with large plagioclase grains and flow banded texture. (d) Hauy 1, fine grained basalt with a quartz vein running horizontally across the image in XPL. (e) SD2 polished section displaying a variety of minerals with rims in a backscatter image. (f) Backscattered electron image of Hauy 1with weathered mineral phases. (g) Backscattered electron image of sample SD1 showing maltese crosses of Fe-Ti oxides. (h) Backscattered electron image of a dolomite-quartz vug in SD1. Mineral abbreviations, Cal: Calcite, Ccp: Chalcopyrite, Chl: Chlorite, Dol: Dolomite, Ilm: Ilmenite, Mag: Magnetite, Ol: Olivine, Plg: Plagioclase, Px: Pyroxene, Py: Pyrite, Qtz: Quartz.

alteration has altered mafic minerals into chlorite, which gives some samples a green hue in plane polarised light (Figure 5c). Carbonate alteration has partially to fully consumed plagioclase grains (Figure 5c), and silicic alteration takes the form of quartz veins and interstitial hydrothermal quartz grains (Figure 5d). One of the samples contains euhedral, "maltese cross" iron-titanium oxides (Figure 5g), carbonate (dolomite and calcite) and quartz filled vugs (Figure 5h).

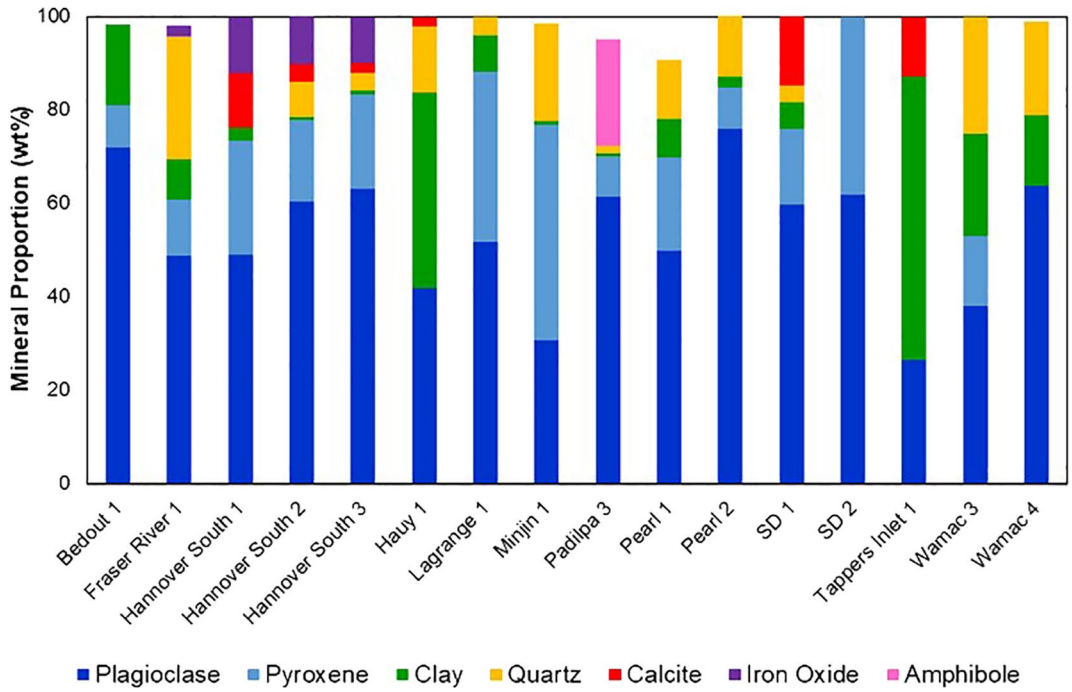

Figure 6. Simplified plot of the XRD mineralogical data.

4.3. Major and Trace Element Geochemistry

The samples have a wide range of SiO_2 (37%–59%), LOI (1.4%–12.6%), total carbon (0.04%–2.69%) and other major element contents (Figure 7; see Supplementary Materials D in Yule & Spandler, 2021), which is consistent with varying intensities of alteration. Loss on ignition (LOI) correlates with K, Ba and Sr indicating these elements have been mobilized during alteration, and the total carbon correlates with the abundance of Ca-Fe-Mg carbonate alteration minerals seen in the thin sections (Figure 5). Traditionally, a total alkali versus silica (TAS) diagram is used to classify volcanic rocks (Figure 8a), but due to the extensive alteration, other major and trace elements are used to determine the composition and origins of the igneous units (Figure 8b). The samples can be divided into two distinct groups based on major element compositions (Figure 7), with Group 1 having higher K_2O, Fe_2O_3, TiO_2, and P_2O_5 and lower MgO than Group 2 samples. Group 2 samples also have a wider range of CaO and MgO contents. These sample groups are spatially distinct with Group 1 distributed exclusively in the offshore basins, whereas Group 2 includes all the onshore Canning Basin samples (Figure 8).

Trace element compositions are used to further distinguish the two sample groups. Group 1 is characterized by relatively high Nb, Zr, Ti and Nb/Y (Figures 8c–8e) and has fairly smooth NMORB-normalised trace element pattern with a positive slope (i.e., LREE-enriched REE patterns) (Figure 9a), which is similar to within plate alkali basalts (Neumann et al., 2011; Pearce, 1996). Group 2 samples are characterized by Nb and Ta negative anomalies and relatively flat (but variably enriched) REE patterns (Figure 9b). Tectonic discrimination based on

Table 2
Summarized Description and Location (UTM 51S) of Thin Section Samples

Sample	Coordinates	Texture	Primary minerals	Alteration minerals	Rock type
SD 1	Y: 7807958	Lathic	Plagioclase, pyroxene, magnetite, olivine, ilmenite	Calcite, quartz, chlorite, chalcopyrite	Dolerite
SD 2	Y: 7807958	Lathic	Plagioclase, pyroxene, magnetite, olivine, spinel	Calcite	Dolerite
Bedout 1	Y: 7979128	Lathic	Plagioclase, pyroxene, magnetite	Chalcopyrite, pyrite, chlorite, calcite	Dolerite
Hauy 1	Y: 7801025	Aphanitic	Plagioclase, pyroxene, magnetite	Chlorite, quartz, calcite, pyrite	Basalt
Tappers Inlet 1	Y: 8135986	Aphanitic	Plagioclase, pyroxene, titanite	Chlorite, calcite, K-feldspar, chalcopyrite	Basalt

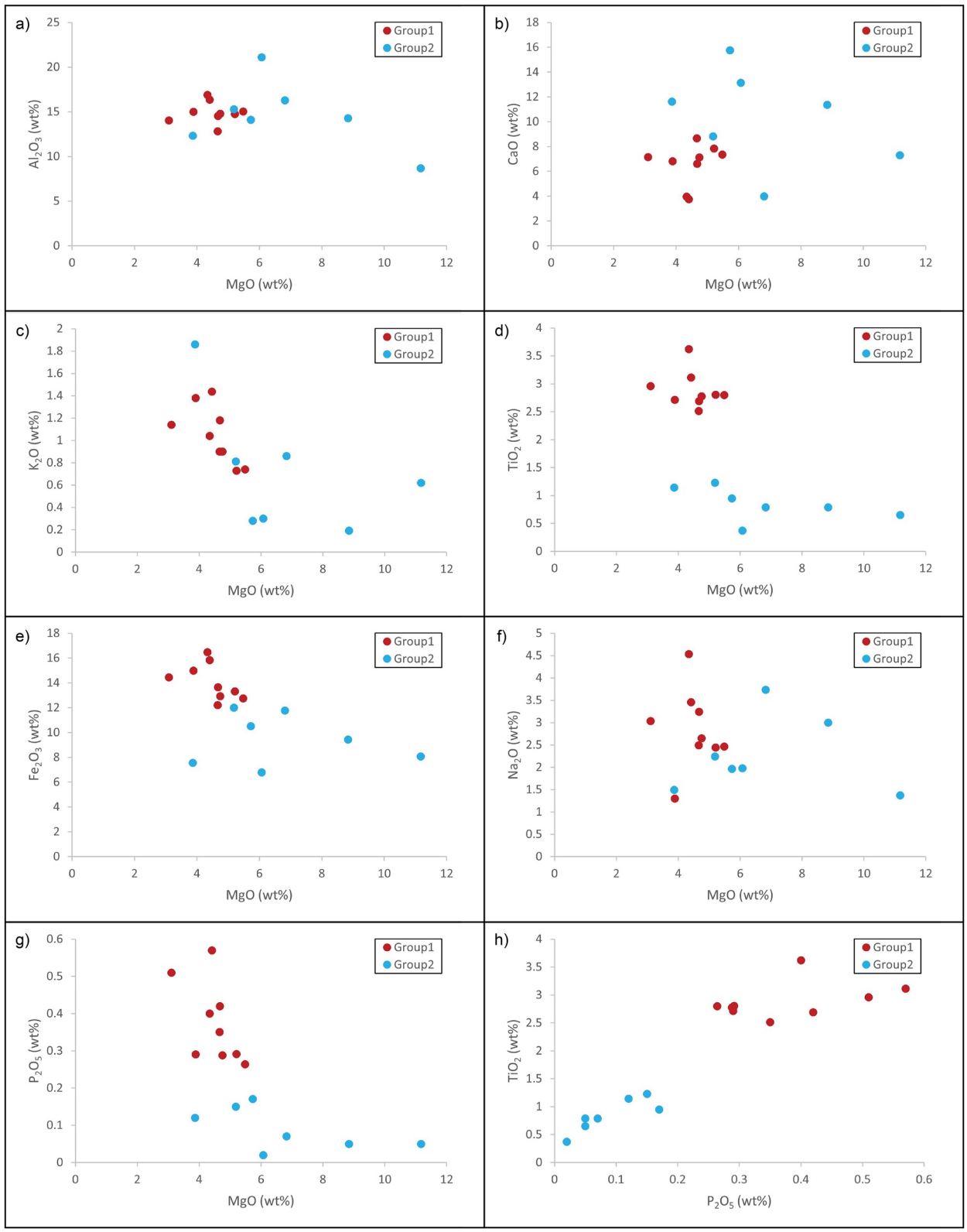

Figure 7. Major element scatter plots of the studied samples. Note the distinction of the two groups, particularly for TiO_2 and P_2O_5 contents.

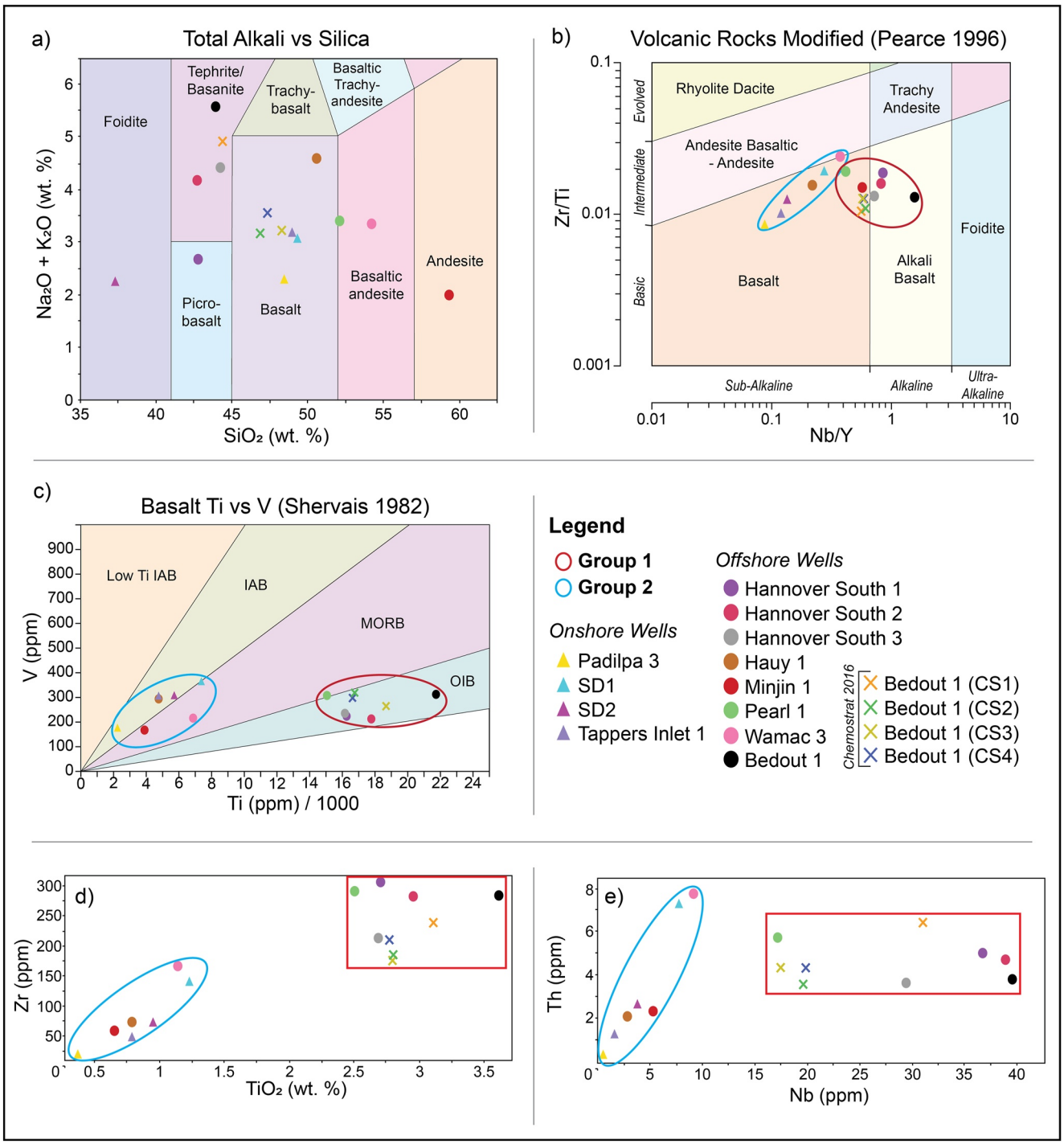

Figure 8. Elemental discrimination diagrams for mafic igneous rocks used to define sample lithology and tectonic setting. (a) TAS diagram. (b) Modified rock classification diagram using Nb/Y and Zr/Ti ratios to remove the effects of alteration. (c) Basalt Ti versus. V diagram to detect crustal contamination from an attenuated continental lithosphere tectonic setting. (d) TiO_2 versus. Zr and (e) Nb versus Th bivariant plots show fractionation and clear distinction between sample groups.

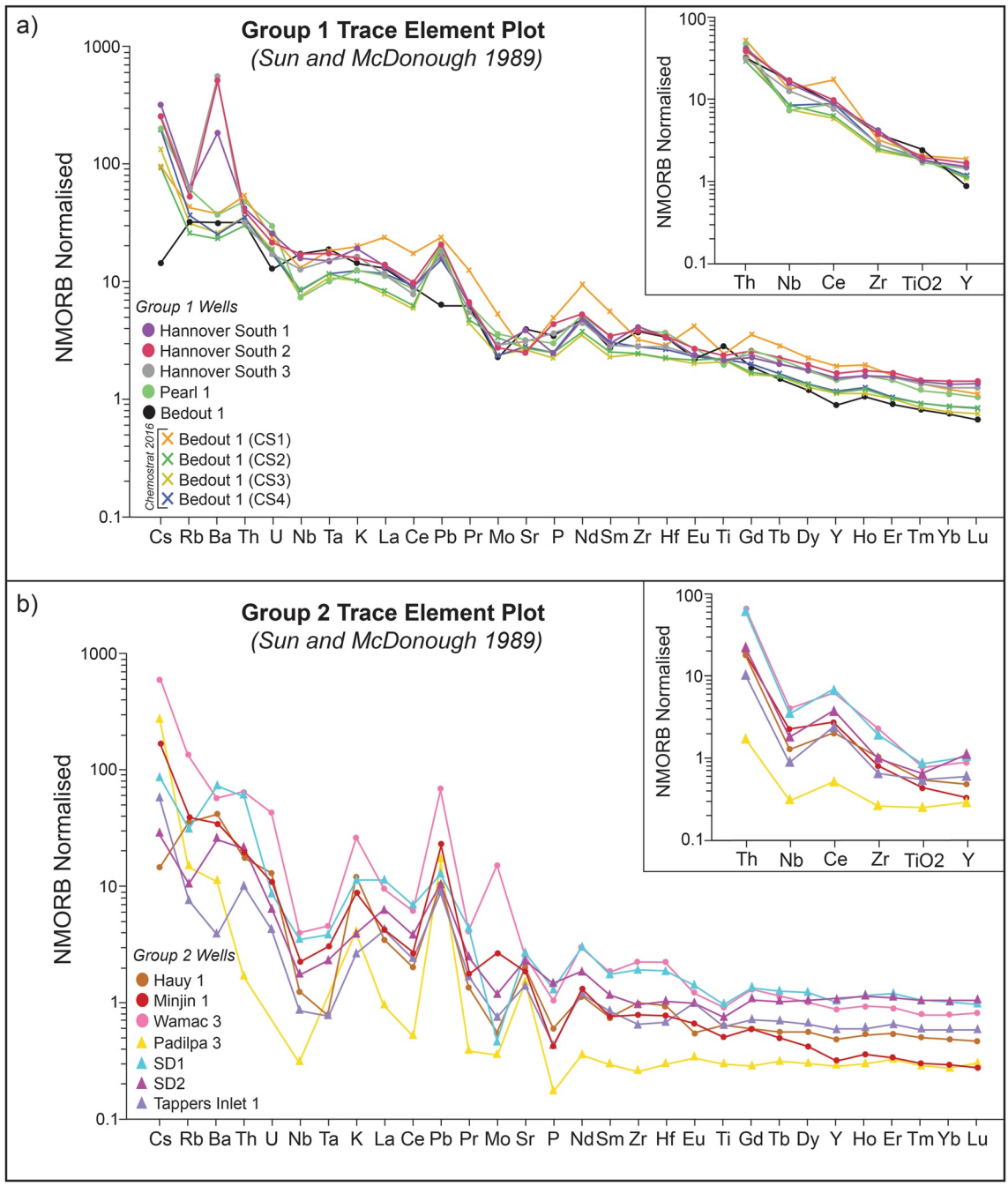

Figure 9. Trace element plots of Group 1 (a) and Group 2 (b) samples. Insets display simplified trace element plots as described in Pearce (1996). Circles represent offshore wells, triangles onshore wells and crosses are data from Chemostrat (2016).

immobile trace elements (Figure 8c) place the Group 1 samples within the ocean island basalt (OIB) field, and Group 2 samples across MORB and island arc basalt (IAB) fields.

5. Discussion

5.1. Is There a LIP or MMP in the Northwest Shelf?

Rollet et al., (2019) proposed the presence of a large igneous province (LIP) on the Northwest Shelf, although that study lacked sufficient data to meet the criteria to formally define a LIP. With our new data, we can now

re-evaluate the validity of a Northwest Shelf LIP. Criteria required to define a LIP, as described by Coffin and Eldholm (1994) and Ernst et al., (2005), include:

1. Flood basalts and extensive dolerite intrusions that collectively have a surface area of >100,000 km^2 and volume of >100,000 km.
2. Bulk of magma emplaced in a 30 Myr period with an emplacement rate reaching at least 1 km^3 per year.
3. Links to regional unconformities, triple junctions, mantle plumes and mass extinctions (Ernst et al., 2005; Glass & Phillips, 2006; Kravchinsky, 2012; Wingate et al., 2004).

A well-established model for LIP formation invokes two major phases of volcanism via mantle plume upwelling and continental rifting (Augland et al., 2019; Black & Gibson, 2019; Burgess et al., 2014; Ernst et al., 2005). In this model, the first phases of magmatism occur prior to rifting and tends to be of alkaline composition. The second magmatic phases, which produce the bulk of the magma, tends to be sub-alkaline in composition and can occur up to 50 Myr later during rifting and after initial doming. The mantle plume which initiates magmatism and rifting also uplifts the overlying crust, resulting in the development of a regional unconformity (Houseman, 1991; Pirajno & Santosh, 2015; Zeyen et al., 1997). Based on the criteria of size, geological setting, geochemistry and timespan of formation, we now assess whether the mafic units of the Northwest Shelf can be classified as a LIP.

5.2. Surface Area and Volume of the Northwest Shelf Mafic Units

Seismic stratigraphic mapping (Figure 10) revealed ~280,000 km^2 of buried mafic igneous material (Figure 3). This value is considered to represent a minimum value as dykes would contribute more volume than is currently measurable and the igneous units may extend further into the North Carnarvon and Browse Basins, which were not fully investigated in this study. This study only mapped the eastern fringe of the North Carnarvon Basin and the results are not representative of the entire basin, including those areas known to contain igneous units of Jurassic-Cretaceous age (Magee & Jackson, 2020; Rohrman, 2013). Additionally, MacNeill et al. (2018) identified ~100,000 km^2 of igneous material in an area that only partially overlaps this study. Using this area estimate of ~280,000 km^2 and inferred thickness, we can calculate an approximate volume of the mafic igneous rocks. Here, we assume an average thickness of 500 m based on the thickest interval drilled by a well (the Hannover South 1 well), which did not penetrate all the way through (see Supplementary Materials Supporting Tables in Yule & Spandler, 2021). 500 m is considered to be a minimum average thickness for several reasons. First, some areas have igneous material up to 10 km thick (Rollet et al., 2019), while other areas may have more igneous material than previously thought due to limitations of seismic data (Schofield et al., 2017). Second, physical limitations of seismic data related to its vertical resolution (greater than 100 m) and attenuation by dense rocks (e.g., mafic igneous rocks), can obscure lower seismic boundaries (Davison et al., 2010; Eide et al., 2017; Schofield et al., 2017). Schofield et al. (2017) determined that up to half the thickness of mafic igneous rocks in modern, high resolution seismic data is undetectable and even more so in lower quality legacy data, such as much of the data used in this study. Third, poor preservation of Paleozoic mafic igneous rocks can remove much of the original material due to its susceptibility to weathering and erosion (Ernst et al., 2005; Wingate et al., 2004; Xu et al., 2014). Considering all these factors, including inferred thicknesses of up to 10 km (MacNeill et al., 2018; Rollet et al., 2019), it is reasonable to suggest the igneous units are more than 500 m thick on average across the study area. Multiplying the 500 m thickness value with the mapped ~280,000 km^2 gives a minimum volume of ~140,000 km^3. Given the connectivity and these surface area and volume estimates, the collective mass of the mafic igneous material within the Northwest Shelf is large enough to meet the size criteria for classification as a LIP.

5.3. Geochemical Signatures

All measured samples are mafic in major element composition, which is consistent with basalt/dolerite descriptions from petrographic analysis. For the most part, the basalts and dolerites belong to Group 1 and Group 2 samples, respectively. The exceptions to this are samples from the Hauy 1 and Pearl 1 wells, where the opposite relationship between geochemical group and rock-type is observed (Figures 5, 7, 8 and 9; see Supplementary Material C and D in Yule & Spandler, 2021). The reason for these differences between the two wells is unknown, but it may relate to localized changes in intrusive versus extrusive nature of the emplacement of the magmatic suites.

10.1029/2021GC010030

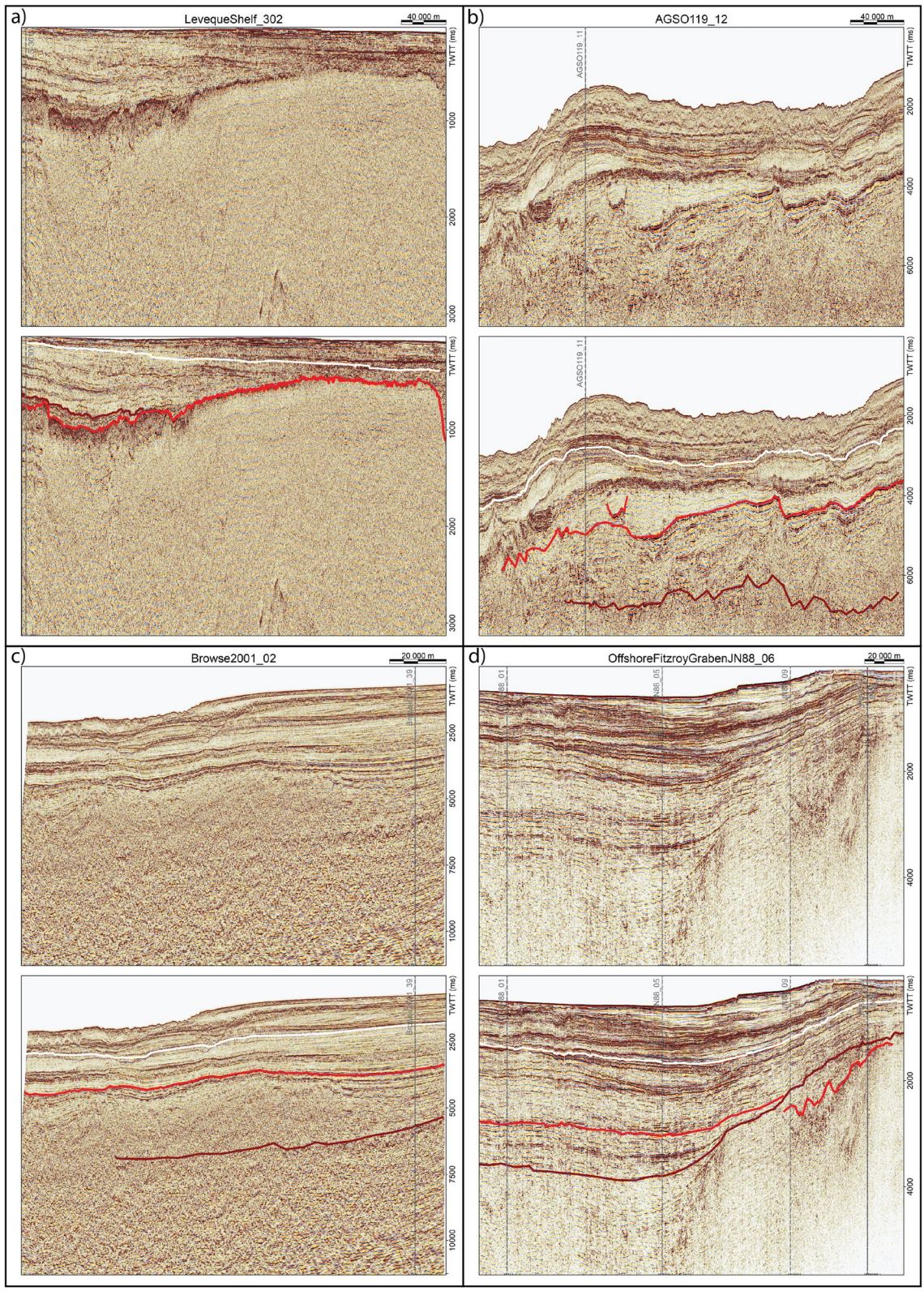

Figure 10.

The geochemistry of mafic igneous rocks are particularly useful as indicators of their tectonic setting of formation, provided care is taken to evaluate chemical changes due to post-emplacement alteration (Pearce, 1996). To avoid issues of alteration on the mafic rocks of the Northwest Shelf, we use alteration immobile elements to provide lithological and tectonic classification of the igneous rocks (Figure 8b). Our results indicate that the Group 1 samples are basalts to alkali basalt, with relative enrichment in incompatible trace elements, as is typical of ocean island-type basalts (Figures 9c and 10). Group 2 rocks are also enriched in incompatible elements compared to MORB, except for relative depletions in Nb, Ta, P, and Ti. This distinctive signature is indicative of volcanic arc basalts (Hawkesworth et al., 1993). However, the Northwest Shelf does not have any association with a subduction-zone tectonic setting (Matthews et al., 2016). The trace element signature may reflect melt generation from a lithospheric mantle source that was previously enriched via ancient convergent margin activity (e.g., Proterozoic Halls Creek Orogen; Tyler et al., 2012), or represents crustal contamination of the magma during migration and emplacement in the upper crust. The latter is supported by the extensive silica and carbonate alteration (Section 4.2); observed in most samples. The mafic igneous rocks from this study share similar geochemical features to mafic magmas that comprise LIPs, including incompatible-element enriched trace element patterns (Figure 9) and Nb, Ti, P and Ta anomalies relative to MORB (Augland et al., 2019; Ernst et al., 2005; Glass & Phillips, 2006; Li et al., 2014; Neumann et al., 2011; Wingate et al., 2004; Xu et al., 2014; Zhang & Zou, 2013). The alkali and incompatible-element enriched feature is attributed to low degree mantle melting and/or melting of enriched mantle sources, while negative Nb, Ta and Ti anomalies have been interpreted to be indicative of crustal contamination by the LIP magmas (Augland et al., 2019; Ernst et al., 2005; Glass & Phillips, 2006; Neumann et al., 2011; Xu et al., 2014; Zhang & Zou, 2013).

5.4. Timing of Magma Emplacement

$^{40}Ar/^{39}Ar$ and $^{40}K/^{39}Ar$ geochronological analyses of igneous units from the Northwest have produced a variety of ages (i.e., Table 1; Gleadow & Duddy, 1984; Reeckmann & Mebberson, 1984; see Supplementary Materials D in Yule & Spandler, 2021). These range from 98 ± 0.5 Ma (see Supplementary Materials D in Yule & Spandler, 2021) to ca. 830 Ma (Reeckmann & Mebberson, 1984). This variety may be attributed to argon loss and excess initial argon (McDougall & Harrison, 2000). Open system behavior relating to alteration, metamorphism and weathering may explain anomalous young ages via post-crystallisation argon loss. Unexpectedly older ages may arise from assumptions in calculating the initial, non-radiogenic isotope composition (i.e., when the initial $^{40}Ar/^{39}Ar$ ratio is greater than atmospheric composition, which is called excess initial argon). Petrographic observations in Section 4.2 indicate a high degree of alteration in the mafic igneous rocks examined in this study (Figure 5), which may partly explain the age variations. Nevertheless, the necessity of future geochronologic work is highlighted by the lack of consensus on the age of this large scale feature. Furthermore, a suite of new ages could facilitate quantitative temporal correlation of isolated occurrences of igneous rocks across the Northwest Shelf.

Although radiogenic isotopic age control is poor, stratigraphic relationships can be used to provide relative temporal constraint. The basaltic and doleritic components have differing stratigraphic positions that meet along the boundary of the north-western offshore Canning Basin (Figures 10 and 11). The basalts are above the Grant Group in the Browse, Roebuck and North Carnarvon Basins (Figures 10b–10d) whereas the dolerites intrude into the Grant Group and lower units in the Canning Basin (Figures 10a and 10d), constraining the stratigraphic age of the dolerites to Permian or older (Figure 11; see Supplementary Materials A in Yule & Spandler, 2021). The basalts overlap more of the Grant Group in the Oobagooma and Willara Sub-basins which may be due to localized subsidence throughout the Paleozoic and Mesozoic (Craig et al., 1984; Müller et al., 2005). Moreover, basalts above the Grant Group in the Canning Basin may be absent due to erosion as the top of the Grant Group is marked by a regional unconformity that persists into the Triassic (Kelman et al., 2013; Luck, 1991; Rollet et al., 2019; Smith et al., 2013; see Supplementary Material A in Yule & Spandler, 2021). Therefore, using these stratigraphic relationships and available geochronological data (Table 1; Gleadow & Duddy, 1984; Reeckmann & Mebberson, 1984), the basalt component is interpreted to have been emplaced with a 50 Myr time window in the

Figure 10. Seismic stratigraphic correlations across the study area. The vertical axis is in milliseconds two-way travel time (TWTT). The white horizon is the top of Mesozoic strata, the brown horizon is the Permian Grant Group and the red horizon represents mafic igneous units. Mafic igneous units above and below the Grant Group are extrusive basalt and intrusive dolerite respectively. (a) Seismic line Leveque Shelf 302 acquired in the North Carnarvon Basin. (b) Seismic line AGSO 119 12 acquired in the Browse Basin. (c) Seismic line Browse 2001 02 acquired in the Roebuck Basin. (d) Seismic line Offshore Fitzroy Graben JN88 06 acquired in the offshore Canning Basin. All other seismic stratigraphic correlations are presented in Supplementary Material A in Yule & Spandler (2021).

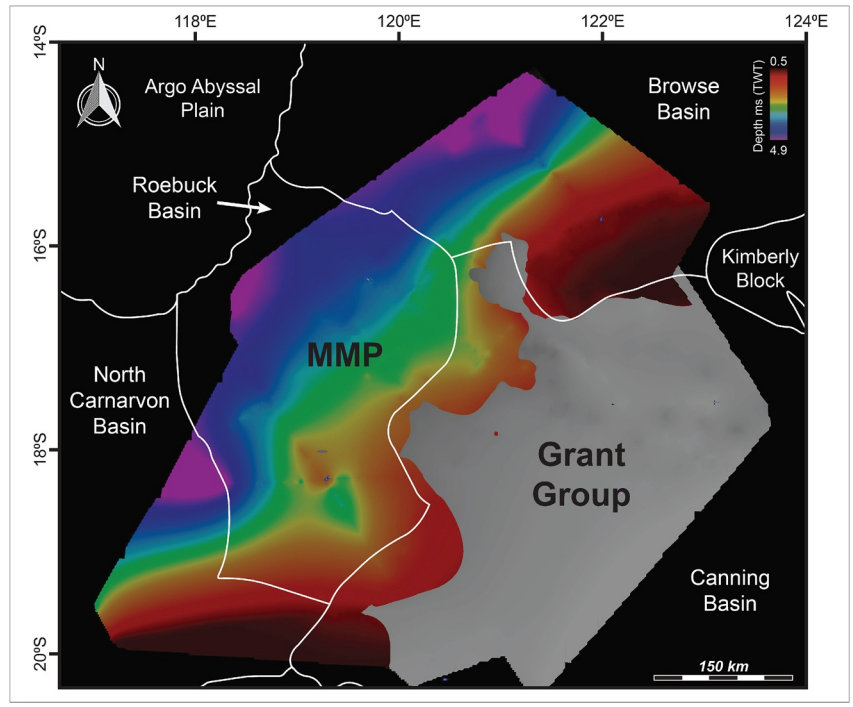

Figure 11. Intersection of the interpolated MMP and Grant Group horizons in 3D. The component of the MMP above the Grant Group can be classified as extrusive basalt and the MMP component beneath the Grant Group as intrusive dolerite. The vertical axis of the MMP is expressed as seconds in two-way travel time (TWT).

Permo-Triassic. The surface area of the basalt component tied to the Permo-Triassic is ~187,000 km^2, which on its own is sufficient to meet a criterion of a LIP. However, using the 500 m minimum thickness, ~93,500 km^3 does not meet LIP volume criteria, but given this is a minimum estimate and the basalt component reaches up to 10 km thick in some areas (Rollet et al., 2019), it is likely that the basalt component meets LIP volume requirements.

Tying the stratigraphic relationships with geochemical findings indicates a significant proportion, if not all, of the igneous rocks were emplaced by a rifting event during the Permo-Triassic period.

Permo-Triassic emplacement is also supported by observations of force folds from igneous intrusions. Force folds are anti-form structures that force strata upward to create space for magma emplacement. Force folds appear above igneous intrusions, do not change the thickness of overlying strata that do not onlap with the intrusion itself, and can be temporally constrained by the oldest onlapping unit (Magee et al., 2013, 2017). Force folds appear to only influence the Permian Grant Group (F78A 13, F79A 01A, F79A 22, Leveque Shelf 198, Leveque Shelf 301, Leveque Shelf 302, Offshore Fitzroy Graben JN88 05, see Supplementary Materials A in Yule & Spandler, 2021) and not Mesozoic strata (Leveque Shelf 113, Leveque Shelf 302 and Wyla 09, see Supplementary Materials A in Yule & Spandler, 2021), which broadly suggests emplacement may have occurred in the Permo-Triassic between the deposition of the Grant Group and Mesozoic units.

Studies from the neighboring North Carnarvon Basin identified a LIP on the Exmouth Plateau and suggested emplacement occurred during the Jurassic to Cretaceous (Magee & Jackson, 2020). Although the Exmouth Plateau LIP does not overlap with the igneous units in this study, it is conceivable that the two magmatic provinces are related (Magee & Jackson, 2020; Rohrman, 2013). Like this study, research from the North Carnarvon Basin lacks geochronological constraint to confidently assign age values to the igneous rocks, but a Jurassic to Cretaceous age should be considered because it coincides with rifting of the Mawgyi Terrane from the Northwest Shelf (Metcalfe, 2006; Müller et al., 2005; Yeates et al., 1984).

In the greater geological context, the event that most likely formed the mafic igneous rocks in the study area was the late Permian - Early Triassic continental break-up of the Cimmerian Block with the Northwest Shelf. Continental break-up is interpreted to have been initiated by a magma plume upwelling under the lithosphere, which thinned

the crust and developed a triple junction (Li & Powell, 2001; Matthews et al., 2016; Rollet et al., 2019). The triple junction formed a NE/SW trending rift zone across the North Carnarvon, Roebuck and Browse Basins and a perpendicular failed rift arm that is now the Oobagooma Sub-basin/Fitzroy Trough (Figure 1; MacNeill et al., 2018). Mantle plumes and triple junctions are often associated with large scale volcanism that occurs in two stages; an initial alkali eruption and a later, but much larger eruption of sub-alkaline magma (Augland et al., 2019; Black & Gibson, 2019; Burgess et al., 2014; Ernst et al., 2005). We identified an alkali group (Group 1) and a sub-alkaline group (Group 2) of mafic rocks that may represent pre-rift and syn-rift magmatic phases, respectively. After large scale rifting events, continental rebound occurs due to the reduction in lithostatic load, leading to uplift and erosion (Houseman, 1991; Pirajno & Santosh, 2015; Zeyen et al., 1997). This uplift may have formed the regional unconformity above the Grant Group and the subsequent erosion of basalts in the Canning Basin (see Supplementary Material A in Yule & Spandler, 2021). Therefore, a Permo-Triassic mantle plume driving continental break-up, voluminous emplacement of two magma types, a regional unconformity, and formation of a triple junction (Houseman, 1991; MacNeill et al., 2018), could be the mechanism that formed a potential LIP on the Northwest Shelf.

5.5. Summary of Characteristics

The mafic igneous rocks examined in this study meet many LIP criteria. Surface area (~280,000 km^2) and volume (~140,000 km^3) estimates of widespread basalt flows and dolerite networks exceed the minimum requirements of a LIP (Coffin & Eldholm, 1994). The Northwest Shelf mafic igneous rocks have both alkaline and subalkaline phases of volcanism (Figures 8 and 9) as is characteristic of LIPs, and contemporary basin wide unconformity and triple junction tectonism is consistent with the lithospheric responses to mantle plume upwelling (MacNeill et al., 2018; Rollet et al., 2019). However, a crucial component to identifying a LIP that is not adequately addressed with our data relates to timescales of magma emplacement. Available geochronological data (Table 1; see Supplementary Material D in Yule & Spandler, 2021) and structural constraints on magma emplacement (Section 5.4), indicate that a significant proportion of magma was emplaced over a relatively short time period across the Permo-Triassic (Gleadow & Duddy, 1984; Reeckmann & Mebberson, 1984). Future studies focusing on geochronology will be needed to determine eruption timing and magma emplacement rates and, hence, test this final criterion for LIP classification.

In summary, current information on the Northwest Shelf mafic igneous units meet most, but not all, of the criteria for LIP classification, but do meet all the criteria for classification as a mafic magmatic province (MMP) (Ernst, 2014). This MMP, herein named the Northwest Shelf MMP, represents a new geological feature that is buried across much of the Northwest Shelf and hence, has important implications for the geology and exploration and resource potential of the Northwest Shelf.

5.6. MMP Implications: Resources and Geological Understanding of the Northwest Shelf

The presence of a buried MMP in the Northwest Shelf has implications for; (a) hidden depocenters; (b) the lack of hydrocarbon deposit discoveries in the Canning Basin; (c) contributions to the end Permian mass extinction event, and; (d) new Ni-Cu-PGE exploration opportunities. Igneous rocks are typically denser than the surrounding sedimentary rocks, which causes seismic wave attenuation that blocks the signal of depocenters below igneous rocks (Davison et al., 2010; Eide et al., 2017; Holford et al., 2013; Schofield et al., 2017). Therefore, a widespread MMP in the Northwest Shelf obscures deep depocenters (see Supplementary Material A in Yule & Spandler, 2021) in areas with poor seismic quality such as the offshore Canning Basin, which limits geological understanding and resource potential. Targeted surveys may reveal more depocenters and improve imaging of the Northwest Shelf MMP, including thinner intrusions.

MMP sills intruding into petroleum systems not only disrupts reservoirs, but can lead to thermal decomposition of hydrocarbons (or carbonates in host sedimentary rocks) and potential release of large volumes of CO_2 into the atmosphere (Augland et al., 2019; Black & Gibson, 2019). The Canning Basin has many known Paleozoic petroleum systems, but none are of sufficient size and integrity to produce large commercial deposits (Burgess & Bowring, 2015; Cadman et al., 1993; Purcell, 1984; Xu et al., 2014). It is conceivable that voluminous mantle plume magma emplacement into the Canning Basin from the Permian to Triassic, may have decimated many of the Palaeozoic hydrocarbon reservoirs (Augland et al., 2019; Black & Gibson, 2019; Burgess et al., 2017).

Release of a large quantity of CO_2 during emplacement of the Northwest Shelf MMP is evident from extensive, interstitial carbonate phases found during petrographic analysis (Figure 5). This CO_2 may have been derived from the crystallizing mafic magma itself or may have been produced by contact metamorphism of carbonate-rich sedimentary host rocks, or their contained hydrocarbons. A major punctuated CO_2 release may have contributed to rapid global climate change such as the end Permian mass extinction (Augland et al., 2019; Burgess et al., 2017; Ernst et al., 2005; Glass & Phillips, 2006; Kravchinsky, 2012; Wingate et al., 2004). Additionally, the Tarim LIP (Li et al., 2014; Xu et al., 2014) may be related to the Northwest Shelf MMP as the Tarim Block rifted from the Northwest Shelf in the Permian (Yang et al., 2013; Zhang & Zou, 2013).

MMPs and/or LIPs are globally recognised for their potential to host significant Ni, Cu and PGE (Wingate et al., 2004) as orthomagmatic sulfide deposits (Pirajno & Hoatson, 2012). These metals are essential for a growing technology market (Bleiwas & Wilburn, 2004), so the onshore Canning Basin may have potential for hosting these resources. The Northwest Shelf, and particularly basalts of the Browse Basin (Rollet et al., 2016), may also be suitable for large scale CO_2 sequestration and storage, as CO_2 can be stored in stable minerals when it reacts with basalt under sediment cover (Goldberg et al., 2008).

6. Conclusion

Analysis of the mafic igneous rocks in the Northwest Shelf has revealed they comprise an interconnected magmatic mass that can be classified as a buried MMP. The only criteria not met for classification as a LIP is eruption timing and calculated magma emplacement rates due to a lack of available geochronological data. Emplacement of the Northwest Shelf MMP has geological and exploration implications for the Northwest Shelf, including a reduction in hydrocarbon potential for some areas, new metalliferous resource possibilities onshore, and potential contributions to the end Permian mass extinction event.

Data Availability Statement

Supplementary material including scripts, raw data, images and additional sample information which are available through Dryad and Zenodo online repositories under a GNU GPLv3 licence (https://doi.org/10.5061/dryad.1c59zw3vx).

Acknowledgments
The authors acknowledge the Aboriginal peoples of Australia as the Traditional Custodians of the lands and waters featured in this research. The authors pay our respects to Elders past and present and we recognise and celebrate the knowledge of Traditional Custodians and their ongoing contributions to science and society. The name "Northwest Shelf" for the mafic magmatic province presented here is temporary and a formal name is forthcoming, awaiting recommendation from the Traditional Custodians of the region. The authors are grateful to Geoscience Australia and the Geological Survey of Western Australia for providing and maintaining publicly available seismic and well data. The authors thank J. Daniell and T. Beveridge for conceptualisation and informal reviews.

References

Augland, L., Ryabov, V., Vernikovsky, V., Planke, S., Polozov, A., Callegaro, S., et al. (2019). The main pulse of the Siberian Traps expanded in size and composition. *Scientific Reports*, *9*(1). https://doi.org/10.1038/s41598-019-54023-2

Austin, J., Foss, C., & Hillan, D. (2014). Advantages and limitations of magnetic and gravity data for mineral exploration undercover. In *Uncover summit 2014*. Adelaide, Australia. Australian Academy of Sciences. Retrieved From http://hdl.handle.net/102.100.100/95297?index=1

Australian Geological Survey Organisation (AGSO), & Geoscience Australia. (2001). *Line drawings of AGSO—Geoscience Australia's regional seismic profile, offshore northern and northwestern Australia*. Canberra: AGSO—Geoscience Australia.

Black, B., & Gibson, S. (2019). Deep carbon and the life cycle of large igneous provinces. *Elements*, *15*(5), 319–324. https://doi.org/10.2138/gselements.15.5.319

Bleiwas, D. I., & Wilburn, D. (2004). *Platinum-group metals: World supply and demand*. USGS. Retrieved from http://pubs.usgs.gov/of/2004/1224/2004-1224.pdf

Blevin, J. E., Boreham, C. J., Summons, R. E., Struckmeyer, H., & Loutit, T. S. (1998). An effective Lower Cretaceous petroleum system on the North West Shelf: Evidence from the Browse Basin. In *The sedimentary basins of Western Australia 2: Proceedings of the petroleum exploration society of Australia symposium* (pp. 397–420). Perth: PESA.

Blevin, J. E., Stephenson, A. E., & West, B. G. (1994). Mesozoic structural development of the Beagle Sub-basin—Implications for the petroleum potential of the northern Carnarvon Basin. In *The sedimentary basins of Western Australia, Proceedings of the petroleum exploration society symposium* (pp. 479–496). PESA.

Brown, S., Boserio, I., Jackson, K., & Spence, K. (1984). The Geological Evolution of the Canning Basin—Implications for petroleum exploration. In P. G. Purcell, (Ed.), *The Canning Basin, WA* (pp. 85–96). Geological Society of Australia/Petroleum Exploration Society of Australia Symposium, Perth.

Burgess, S., Bowring, S., & Shen, S. (2014). High-precision timeline for Earth's most severe extinction. *Proceedings of the National Academy of Sciences*, *111*(9), 3316–3321. https://doi.org/10.1073/pnas.1317692111

Burgess, S., Muirhead, J., & Bowring, S. (2017). Initial pulse of Siberian Traps sills as the trigger of the end-Permian mass extinction. *Nature Communications*, *8*(1). https://doi.org/10.1038/s41467-017-00083-9

Burgess, S. D., & Bowring, S. A. (2015). High-precision geochronology confirms voluminous magmatism before, during, and after Earth's most severe extinction. *Science Advances*, *1*, e1500470. https://doi.org/10.1126/sciadv.1500470

Cadman, S. J., Pain, L., Vuckovic, V., & le Poidevin, S. R. (1993). *Australian Petroleum Accumulations Report 9, 1993*. Bureau of Resource Sciences.

Chemostrat (2016). *Chemostratigraphic analysis of Bedout-1*. Retrieved From http://www.ga.gov.au/nopims

Coffin, M., & Eldholm, O. (1994). Large igneous provinces: Crustal structure, dimensions, and external consequences. *Reviews of Geophysics*, *32*(1), 1. https://doi.org/10.1029/93rg02508

Cortez, M., & Cetale Santos, M. (2016). Seismic interpretation, attribute analysis, and illumination study for targets below a volcanic-sedimentary succession, Santos Basin, offshore Brazil. *Interpretation*, *4*(1), SB37–SB50. https://doi.org/10.1190/int-2015-0097.1

Craig, J., Downey, J., Gibbs, A., & Russell, J. (1984). The application of landsat imagery in structural interpretation of the Canning Basin, W.A. In (Ed.), *The Canning Basin, WA* (pp. 57–72). Geological Society of Australia/Petroleum Exploration Society of Australia Symposium, Perth.

Davison, I., Stasiuk, S., Nuttall, P., & Keane, P. (2010). Sub-basalt hydrocarbon prospectivity in the Rockall, Faroe–Shetland and Møre basins, NE Atlantic. *Geological Society, London, Petroleum Geology Conference Series*, *7*(1), 1025–1032. https://doi.org/10.1144/0071025

DiCaprio, L., Gurnis, M., & Müller, R. D. (2009). Long-wavelength tilting of the Australian continent since the late cretaceous. *Earth and Planetary Science Letters*, *278*(3), 175–185. https://doi.org/10.1016/j.epsl.2008.11.030

Eide, C., Schofield, N., Lecomte, I., Buckley, S., & Howell, J. (2017). Seismic interpretation of sill complexes in sedimentary basins: Implications for the sub-sill imaging problem. *Journal of the Geological Society*, *175*(2), 193–209. https://doi.org/10.1144/jgs2017-096

Ernst, R. (2014). *Large igneous provinces*. Cambridge University Press. https://doi.org/10.1017/CBO9781139025300

Ernst, R., Buchan, K., & Campbell, I. (2005). Frontiers in large igneous province research. *Lithos*, *79*(3–4), 271–297. https://doi.org/10.1016/j.lithos.2004.09.004

Ernst, R. E., & Buchan, K. L. (2001). Large mafic magmatic events through time and links to mantle-plume heads. In R. E. Ernst, & K. L. Buchan, (Eds.), *Mantle plumes: Their identification through time* (Vol. 352). https://doi.org/10.1130/0-8137-2352-3.483

Frogtech (2014). *Phanerozoic OZ SEEBASE v2 GIS. Bioregional assessment source dataset*. Retrieved From http://data.bioregionalassessments.gov.au/dataset/26e0fbd9-d8d0-4212-be52-ca317e27b3bd

Geoscience Australia. (2019). *Regional geology of the Browse Basin*. Retrieved From https://www.ga.gov.au/scientific-topics/energy/province-sedimentary-basin-geology/petroleum/acreagerelease/browse

Glass, L., & Phillips, D. (2006). The Kalkarindji continental flood basalt province: A new Cambrian large igneous province in Australia with possible links to faunal extinctions. *Geology*, *34*(6), 461. https://doi.org/10.1130/g22122.1

Gleadow, A. J. W., & Duddy, I. R. (1984). Fission track dating and thermal history analysis of apatites from wells in the Northwest Canning Basin. In P. G. Purcell, (Ed.), *The Canning Basin, WA* (pp. 377–387). Geological Society of Australia/Petroleum Exploration Society of Australia Symposium, Perth.

Goldberg, D. S., Takahashi, T., & Slagle, A. L. (2008). Carbon dioxide sequestration in deep-sea basalt. *Proceedings of the National Academy of Sciences of the United States of America*. https://doi.org/10.1073/pnas.0804397105

GSWA (2017). *Summary of petroleum prospectivity: Canning Basin*. Retrieved From http://www.dmp.wa.gov.au/Documents/Petroleum/Petroleum-SummaryProspectivityCanningBasin2017.pdf

Hackney, R., Goodwin, J., Hall, L., Higgins, K., Holzrichter, N., Johnston, S., et al. (2015). Potential-field data in integrated Frontier basin geophysics: Successes and challenges on Australia's continental margin. *Marine and Petroleum Geology*, *59*, 611–637. https://doi.org/10.1016/j.marpetgeo.2014.01.014

Hashimoto, T., Bailey, A., Chirinos, A., & Carr, L. K. (2018). *Onshore basin inventory volume 2: The Canning, Perth and Officer basins*. Geoscience Australia. https://doi.org/10.11636/Record.2018.018

Hawkesworth, C. J., Gallagher, K., Hergt, J. M., & McDermott, F. (1993). Mantle and Slab Contributions in ARC Magmas. *Annual Review of Earth and Planetary Sciences*, *21*(1), 175–204. https://doi.org/10.1146/annurev.ea.21.050193.001135

Heirtzler, J. R., Cameron, P., Cook, P. J., Powell, T., Roeser, H. A., Sukardi, S., & Veevers, J. J. (1978). The Argo abyssal plain. *Earth and Planetary Science Letters*, *41*(1), 21–31. https://doi.org/10.1016/0012-821x(78)90038-9

Holford, S. P., Schofield, N., Jackson, C., Magee, C., Green, P. F., & Duddy, I. R. (2013). Impacts of igneous intrusions on source and reservoir potential in prospective sedimentary basins along the western Australian continental margin. In M. Keep, & S. J. Moss (Eds.),, (Eds), *The sedimentary basins of Western Australia IV*. Perth, WA: Proceedings of the petroleum exploration Society of Australia Symposium.

Houseman, G. (1991). The triple-junction structure of mantle plumes and continental rifting. *Exploration Geophysics*, *22*(1), 195–198. https://doi.org/10.1071/eg991195

Keep, M., Harrowfield, M., & Crowe, W. (2007). The Neogene tectonic history of the Northwest Shelf, Australia. *Exploration Geophysics*, *38*(3), 151–174. https://doi.org/10.1071/EG07022

Kelman, A. P., Nicoll, R. S., Kennard, J. M., Mory, A. J., Mantle, D. J., le Poidevin, S., et al. (2013). *Northern Carnarvon Basin Biozonation and Stratigraphy* (Vol. 36). Geoscience Australia.

Kravchinsky, V. (2012). Paleozoic large igneous provinces of Northern Eurasia: Correlation with mass extinction events. *Global and Planetary Change*, *86–87*, 31–36. https://doi.org/10.1016/j.gloplacha.2012.01.007

Kutovaya, A., Kroeger, K., Seebeck, H., Back, S., & Littke, R. (2019). Thermal effects of magmatism on surrounding sediments and petroleum systems in the northern offshore Taranaki Basin, New Zealand. *Geosciences*, *9*(7), 288. https://doi.org/10.3390/geosciences9070288

Li, D., Yang, S., Chen, H., Cheng, X., Li, K., Jin, X., et al. (2014). Late Carboniferous crustal uplift of the Tarim plate and its constraints on the evolution of the Early Permian Tarim Large igneous province. *Lithos*, *204*, 36–46. https://doi.org/10.1016/j.lithos.2014.05.023

Li, Z., Bogdanova, S., Collins, A., Davidson, A., De Waele, B., Ernst, R., et al. (2008). Assembly, configuration, and break-up history of Rodinia: A synthesis. *Precambrian Research*, *160*(1–2), 179–210. https://doi.org/10.1016/j.precamres.2007.04.021

Li, Z. X., & Powell, C. M. (2001). An outline of the palaeogeographic evolution of the Australasian region since the beginning of the Neoproterozoic. *Earth-Science Reviews*, *53*(3), 237–277. https://doi.org/10.1016/S0012-8252(00)00021-0

Luck, G. R. (1991). *Offshore Canning Basin: Time structure maps*. Geological Survey of Western Australia. Retrieved From https://dmpbookshop.eruditetechnologies.com.au/product/offshore-canning-basin-time-structure-maps-set-of-24.do

Luke, B., Calderón-Macías, C., Stone, R., & Huynh, M. (2003). Non-uniqueness in inversion of seismic surface-wave data. In *Conference proceedings, 16th EEGS symposium on the application of geophysics to engineering and environmental problems*. European Association of Geoscientists & Engineers. https://doi.org/10.3997/2214-4609-pdb.190.sur05

MacNeill, M., Marshall, N., & McNamara, C. (2018). New Insights into a major Early-Middle Triassic Rift Episode in the NW Shelf of Australia. *ASEG Extended Abstracts*, *2018*(1), 1–5. https://doi.org/10.1071/aseg2018abm3_3b

Magee, C., Briggs, F., & Jackson, C. (2013). Lithological controls on igneous intrusion-induced ground deformation. *Journal of the Geological Society*, *170*(6), 853–856. https://doi.org/10.1144/jgs2013-029

Magee, C., & Jackson, C. (2020). Seismic reflection data reveal the 3D structure of the newly discovered Exmouth Dyke Swarm, offshore NW Australia. *Solid Earth*, *11*(2), 579–606. https://doi.org/10.5194/se-11-579-2020

Magee, C., Jackson, C., Hardman, J., & Reeve, M. (2017). Decoding sill emplacement and forced fold growth in the Exmouth Sub-basin, offshore northwest Australia: Implications for hydrocarbon exploration. *Interpretation*, *5*(3), SK11–SK22. https://doi.org/10.1190/int-2016-0133.1

Magee, C., Muirhead, J., Karvelas, A., Holford, S., Jackson, C., Bastow, I., et al. (2016). Lateral magma flow in mafic sill-complexes. *Acta Geologica Sinica*, *90*(s1), 4–5. https://doi.org/10.1111/1755-6724.12848

Matthews, K. J., Maloney, K. T., Zahirovic, S., Williams, S. E., Seton, M., & Müller, R. D. (2016). Global plate boundary evolution and kinematics since the late Palaeozoic. *Global and Planetary Change*, *146*, 226–250. https://doi.org/10.1016/j.gloplacha.2016.10.002

McClay, K., Scarselli, N., & Jitmahantakul, S. (2013). Igneous intrusions in the Carnarvon Basin, NW Shelf, Australia. In *The sedimentary basins of Western Australia IV*. Proceedings of the Petroleum Exploration Society of Australia Symposium.

McDougall, I., & Harrison, T. (2000). Geochronology and thermochronology by the 40Ar/39Ar method. *Journal of Petrology*, *41*(12), 1823–1824. https://doi.org/10.1093/petrology/41.12.1823

Merdith, A. S., Williams, S. E., Collins, A. S., Tetley, M. G., Mulder, J. A., Blades, M. L., et al. (2021). Extending full-plate tectonic models into deep time: Linking the Neoproterozoic and the Phanerozoic. *Earth-Science Reviews*, *214*, 103477. https://doi.org/10.1016/j.earscirev.2020.103477

Metcalfe, I. (2006). Palaeozoic and Mesozoic tectonic evolution and palaeogeography of East Asian crustal fragments: The Korean peninsula in context. *Gondwana Research*, *9*(1), 24–46. https://doi.org/10.1016/j.gr.2005.04.002

Mory, A., & Haines, P. (2013). A Paleozoic perspective of Western Australia. In *West Australian basins symposium 2013*.

Müller, R. D., Goncharov, A., & Kritski, A. (2005). Geophysical evaluation of the enigmatic Bedout basement high, offshore north western Australia. *Earth and Planetary Science Letters*, *237*(1), 264–284. https://doi.org/10.1016/j.epsl.2005.06.014

National Offshore Petroleum Information Management System (NOPIMS) (2019). Retrieved From https://www.ga.gov.au/nopims

Neumann, E., Svensen, H., Galerne, C., & Planke, S. (2011). Multistage evolution of dolerites in the Karoo large igneous province, Central South Africa. *Journal of Petrology*, *52*(5), 959–984. https://doi.org/10.1093/petrology/egr011

Nicoll, R. S., Kennard, J. M., Kelman, A. P., Mantle, D. J., Laurie, J. R., & Edwards, D. S. (2009). *Browse basin biozonation and stratigraphy*. Retrieved From http://www.ga.gov.au/webtemp/image_cache/GA14405.pdf

Pearce, J. A. (1996). A user's guide to basalt discrimination diagrams. In D. A. Wyman, (Ed.), *Trace element geochemistry of volcanic rocks: Applications for massive sulphide exploration*. (Vol. 12, pp. 79–113). Geological Association of Canada.

Phillips, T. B., Magee, C., Jackson, C. A. L., & Bell, R. E. (2018). Determining the three-dimensional geometry of a dike swarm and its impact on later rift geometry using seismic reflection data. *Geology*, *46*(2), 119–122. https://doi.org/10.1130/G39672.1

Pirajno, F., & Hoatson, D. M. (2012). A review of Australia's large igneous provinces and associated mineral systems: Implications For mantle dynamics through geological time. *Ore Geology Reviews*, *48*, 2–54. https://doi.org/10.1016/j.oregeorev.2012.04.007

Pirajno, F., & Santosh, M. (2015). Mantle plumes, supercontinents, intracontinental rifting and mineral systems. *Precambrian Research*, *259*, 243–261. https://doi.org/10.1016/j.precamres.2014.12.016

Purcell, P. (1984). The Canning Basin, W.A.—An Introduction. In P. G. Purcell, (Ed.), *The Canning Basin, WA* (pp. 3–19). Geological Society of Australia/Petroleum Exploration Society of Australia Symposium, Perth.

Reeckmann, S. A., & Mebberson, A. J. (1984). Igneous intrusions in the Northwest Canning Basin and their impact on oil exploration. In P. G. Purcell (Ed.), *The Canning Basin, WA* (pp. 85–96). Geological Society of Australia/Petroleum Exploration Society of Australia Symposium, Perth.

Rohrman, M. (2013). Intrusive large igneous provinces below sedimentary basins: An example from the Exmouth Plateau (NW Australia). *Journal of Geophysical Research: Solid Earth*, *118*(8), 4477–4487. https://doi.org/10.1002/jgrb.50298

Rohrman, M., & Lisk, M. (2010). Geophysical delineation of volcanics and intrusives offshore NW Australia using global analogues. *ASEG Extended Abstracts*, *2010*, 1–3. https://doi.org/10.1071/ASEG2010ab136

Rollet, N., Abbott, S. T., Lech, M. E., Romeyn, R., Grosjean, E., Edwards, D. S., & Totterdell, J. M. (2016). *A regional assessment of CO_2 storage potential in the Browse Basin: Results of a study undertaken as part of the national CO_2 infrastructure plan*. Geoscience Australia.

Rollet, N., Shi, Z., Morse, M., Poudjom Djomani, Y., & Gunning, M. (2019). *Crustal structure and distribution of volcanics in the Northern Carnarvon and Roebuck basins, central Australian Northwest Shelf*. Geoscience Australia. https://doi.org/10.11636/Record.2019.022

Schofield, N., Holford, S., Millett, J., Brown, D., Jolley, D., Passey, S., et al. (2017). Regional magma plumbing and emplacement mechanisms of the Faroe-Shetland Sill Complex: Implications for magma transport and petroleum systems within sedimentary basins. *Basin Research*, *29*(1), 41–63. https://doi.org/10.1111/bre.12164

Schutter, S. (2003). Hydrocarbon occurrence and exploration in and around igneous rocks. *Geological Society, London, Special Publications*, *214*(1), 7–33. https://doi.org/10.1144/gsl.sp.2003.214.01.02

Slezak, P., & Spandler, C. (2020). Petrogenesis of the Gifford creek carbonatite complex, Western Australia. *Contributions to Mineralogy and Petrology*, *175*(3). https://doi.org/10.1007/s00410-020-1666-3

Smith, S., Tingate, P., Griffths, C., & Hull, J. (1999). The structural development and petroleum potential of the roebuck basin. *The APPEA Journal*, *39*(1), 364. https://doi.org/10.1071/aj98020

Smith, T., Edwards, D., Kelman, A., Laurie, J., le Poidevin, S., & Nicoll, R. (2013). *Canning Basin Biozonation and Stratigraphy Chart* (Vol. 31). Geoscience Australia.

Sun, W., Zhou, B., Hatherly, P., & Fu, L. (2010). Seismic wave propagation through surface basalts—Implications for coal seismic surveys. *Exploration Geophysics*, *41*(1), 1–8. https://doi.org/10.1071/eg09015

Symonds, P. A., Planke, S., Frey, O., & Skogseid, J. (1998). Volcanic evolution of the Western Australian continental margin and its implications for basin development. In P. G. Purcell, & R. R. Purcell (Eds.), *The sedimentary basins of Western Australia 2: Proceedings of the PESA Symposium*. (pp. 33–54). Petroleum Exploration Society.

Totterdell, J. M., Hall, L., Hashimoto, T., Owen, K., & Bradshaw, M. T. (2014). *Petroleum geology inventory of Australia's offshore frontier basins*. Geoscience Australia. https://doi.org/10.11636/Record.2014.009

Tyler, I. M., Hocking, R. M., & Haines, P. W. (2012). Geological evolution of the Kimberley region of Western Australia. *Episodes*, *35*(1), 298–306. https://doi.org/10.18814/epiiugs/2012/v35i1/029

Western Australia Petroleum Information Management System (WAPIMS) (2019). Retrieved From https://wapims.dmp.wa.gov.au/wapims

Wingate, M., Pirajno, F., & Morris, P. (2004). Warakurna large igneous province: A new Mesoproterozoic large igneous province in west-central Australia. *Geology*, *32*(2), 105. https://doi.org/10.1130/g20171.1

Xu, Y., Wei, X., Luo, Z., Liu, H., & Cao, J. (2014). The Early Permian Tarim large igneous province: Main characteristics and a plume incubation model. *Lithos*, *204*, 20–35. https://doi.org/10.1016/j.lithos.2014.02.015

Yang, S., Chen, H., Li, Z., Li, Y., Yu, X., Li, D., & Meng, L. (2013). Early Permian Tarim large igneous province in Northwest China. *Science China Earth Sciences*, *56*(12), 2015–2026. https://doi.org/10.1007/s11430-013-4653-y

Yeates, A. N., Gibson, D. L., Towner, R., & Crowe, R. W. A. (1984). *Regional geology of the onshore Canning Basin, W.A. The Canning Basin* (pp. 23–55). Geological Society of Australia/Petroleum Exploration Society of Australia Symposium.

Yilmaz, Ö. (2001). *Seismic data analysis: Processing, inversion, and interpretation of seismic data*. Society of Exploration Geophysicists.

Yule, C., & Daniell, J. (2018). The development of a seamless onshore/offshore seismic stratigraphic model of the Canning Basin, Northwest Shelf, Australia. *SEG Global Meeting Abstracts*, 50–53. https://doi.org/10.1190/SEGJ2018-014.1

Yule, C., & Daniell, J. (2019). New insights into the offshore Canning Basin using a seamless onshore/offshore stratigraphic model. *ASEG Extended Abstracts*, *2019*(1), 1–5. https://doi.org/10.1080/22020586.2019.12073038

Yule, C., & Spandler, C. (2021). *Geophysical and geochemical evidence for a new mafic magmatic province within the Northwest Shelf of Australia*. https://doi.org/10.5061/dryad.1c59zw3vx

Zeyen, H., Volker, F., Wehrle, V., Fuchs, K., Sobolev, S., & Altherr, R. (1997). Styles of continental rifting: Crust-mantle detachment and mantle plumes. *Tectonophysics*, *278*(1–4), 329–352. https://doi.org/10.1016/s0040-1951(97)00111-x

Zhang, C., & Zou, H. (2013). Comparison between the Permian mafic dykes in Tarim and the western part of Central Asian Orogenic Belt (CAOB), NW China: Implications for two mantle domains of the Permian Tarim Large Igneous Province. *Lithos*, *174*, 15–27. https://doi.org/10.1016/j.lithos.2012.11.010